THE UNIVERSITY OF MICHIGAN

INDUSTRY PROGRAM OF THE COLLEGE OF ENGINEERING

INITIAL PHASES OF DAMAGE TO TEST SPECIMENS IN A CAVITATING VENTURI AS AFFECTED BY FLUID AND MATERIAL PROPERTIES AND CAVITATION REGIME

F. G. Hammitt
L. L. Barinka
M. J. Robinson
R. D. Pehlke
C. A. Siebert

December, 1963

IP-644

ACKNOWLEDGMENTS

The authors wish to acknowledge the financial support of NASA for the majority of the work herein discussed. In addition, financial support for some of the tests was provided by Pratt and Whitney Division of United Aircraft Corp.

The authors would also like to thank the following research personnel of The University of Michigan for their assistance: K. Aksus, V. Biss, H. Ring, E. Rupke, J. Brigham, Y. Sozusen, E. Shippey, W. Smith, R. Ivany.

ABSTRACT

The detailed characteristics of pitting in the early phases of cavitation damage incurred by test specimens inserted into the diffusing portion of a cavitating venturi are shown pictorially and discussed in terms of degree of cavitation, fluid, material, duration and velocity effects. Quantitative damage results are presented from these tests for mercury and water as test fluids, and for a variety of test materials. Various possible damage correlating parameters are discussed and examined.

TABLE OF CONTENTS

		Page
ACKNOWLEDGMENTS		ii
ABSTRACT		iii
LIST OF TABLES		v
LIST OF FIGURES		vi
I.	INTRODUCTION	1
II.	PITTING CHARACTERISTICS AS AFFECTED BY FLOW, FLUID AND MATERIAL PARAMETERS	8
	A. Degree of Cavitation Effects	8
	B. Fluid Effects	18
	C. Test Material Effects	24
III.	QUANTITATIVE DAMAGE DATA	38
	A. Degree of Cavitation Effects	38
	B. Throat Velocity	40
	C. Duration Effects	42
	D. Fluid and Material Effects	43
IV.	CORRELATION WITH MATERIAL MECHANICAL PROPERTIES	50
	A. Theoretical Considerations	50
	B. Experimental Results	52
V.	CONCLUSIONS	56
VI.	REFERENCES	58
VII.	APPENDIX - SPECIFICATION OF CAVITATION CONDITIONS	59

LIST OF TABLES

Table		Page
I	Typical Mechanical Properties of Materials Tested....	9
II	Comparison of Sizes and Percent Circular Pits on Mercury Samples.....	21
III	Comparison of Sizes and Percent Circular Pits on Water Samples.....	22
IV	Comparative Size Distribution of Pits in Mercury and Water.....	23
V	Data on Surface Finish as a Cavitation Damage Parameter.....	25

LIST OF FIGURES

Figure		Page
1	Drawing of the Damage Test Venturi Showing Location of Specimens, Specimen Holders, and Cavitation Termination Points.....	2
2	Schematic Drawing of Overall Mercury Loop Layout.....	3
3	Schematic Drawing of Overall Water Loop Layout.....	4
4	(a) Drawing of Test Specimen, (b) Photograph of Test Specimen, Showing Polished Surface.....	5
5	Normalized Axial Pressure Profiles for Several Cavitation Conditions with Water (1/2 inch venturi test section No. II).....	7
6	Cavitated Surface of Stainless Steel Specimen Number 84-3 for "Visible Initiation" Cavitation Condition in Mercury at a Throat Velocity of 34 feet/second. Surface was Etched Before Testing. Mag. 37-1/2 X. (a) 6 hours duration, (b) 15 hours duration.....	10
7	Cavitated Surface of Stainless Steel Specimen Number 107-3 for "Nose" Cavitation Condition in Mercury at a Throat Velocity of 34 feet/second. Surface was Etched Before Testing. Mag. 37-1/2 X. (a) 6 hours duration and, (b) 10 hours duration.....	11
8	Cavitated Surface of Stainless Steel Sample Number 71-3 for "Standard" Cavitation Condition in Mercury at a Throat Velocity of 34 feet/second. Surface was Etched Before Testing. Mag. 37-1/2 X. (a) 6 hours duration and, (b) 10 hours duration.....	12
9	Cavitated Surface of Stainless Steel Sample Number 116-3 for "Back" Cavitation Condition in Mercury at a Throat Velocity of 34 feet/second. Surface was Etched Before Testing. Mag. 37-1/2 X. (a) 6 hours duration and, (b) 10 hours duration.....	13
10	Cavitated Surface of Stainless Steel Specimen Number 84-3 for "Visible Initiation" Cavitation Condition in Mercury at a Throat Velocity of 34 feet/second. Mag. 37-1/2 X. (a) Duration 25 hours, (b) same as (a) but Specimen Number 107-3 and "Nose" Cavitation Condition.....	14

LIST OF FIGURES CONT'D

Figure		Page
11	(a) Cavitated Surface of Specimen Number 84-3 for "Visible Initiation" in Mercury at a Throat Velocity of 34 feet/second. Mag. 37-1/2. 10 hour duration. (b) Cavitated Surface of Stainless Steel Specimen Number 99-3 for Same Conditions as (a).....	15
12	Cavitated Surface of Stainless Steel Specimens for "Standard" Cavitation Condition in Water at a Throat Velocity of 64.7 feet/second. Mag. 37-1/2 X. (a) Sample 4-3 at 191 hours duration and, (b) Sample 5-3 at 191 hours duration.....	19
13	Cavitated Surface of Sample Number 55-3 Showing Elongated Pits in the Direction of Flow, Duration 1 Hour, Mag. 120 X. Actual Width of View Shown is Approximately 46.5 mils.....	27
14	Cavitation Pit in Columbium-1% Zirconium After 40 Hours Exposure Showing Wake Formation. Actual Width of View Shown in Approximately 46.5 mils.....	27
15	Macrograph of Cavitated Surface of Carbon Steel Samples Numbers 64-1 and 65-1 for "Nose" Cavitation Condition in Mercury at a Throat Velocity of 34 feet/second. Outside Samples are Undamaged New Samples for Comparison. Mag. 4 X. (a) 4 hours duration and, (b) 7 hours duration.....	30
16	Same as Figure 15 Except, (a) 17 hours duration and, (b) 37 hours duration.....	31
17	Same as Figure 15 Except, (a) 77 hours duration and, (b) 100 hours duration.....	32
18	Magnified Picture of Damage Cut-Off Region in Figure 15(a), (a) Sample 64-1 and, (b) Sample 65-1. Mag. 25X..	34
19	Macrograph of Cavitated Surface of Stainless Steel Samples Numbers 47-3 and 48-3 for "Standard " Cavitation Condition in Mercury at a Throat Velocity of 34 feet/second. Undamaged Samples Included for Comparison. Mag. 4 X. (a) 17 hours duration and, (b) 47 hours duration...	35

LIST OF FIGURES CONT'D

Figure		Page
20	Macrograph of Numbered Side of Sample Number Cb-1 Zr 20 After 50 hours Exposure to "Nose" Cavitation Condition in Mercury at a Throat Velocity of 48 feet/second. Mag. 4 X.....	36
21	Microsection Through Gross Damage Area on Numbered Side of Sample Number Cb-1 Zr 20 as Shown in Figure 20. Etched Mag. 100 X. Actual Width of View Shown in Approximately 46.5 mils.....	36
22	Microsection Through Cavitation Pit on Sample Number Cb-Ar 20, After 50 Hours Exposure to Cavitation Showing Material Microstructure. Etched. Mag. 1000 X Actual Width of View Shown in About 5 mils.....	37
23	Actual Specific Volume Loss vs Cavitation Condition for Constant Times for Stainless Steel in Mercury.....	39
24	Actual Specific Volume Loss vs Throat Velocity for Constant Time and Various Cavitation Conditions for Stainless Steel in Mercury.....	41
25	Mean Depth of Penetration vs Time for Stainless Steel Cavitated in Water.....	44
26	Mean Depth of Penetration vs Time for Various Materials and Velocities in Mercury.....	45
27	Actual Specific Volume Loss vs Time for Different Sample Materials in Mercury.....	47
28	Actual Specific Volume Loss vs Time for Different Sample Materials in Mercury.....	48
29	Normalized Cavitation Damage vs Tensile Strength Comparison of Mercury and Water Data.....	53
30	Normalized Cavitation Damage vs Strain Energy to Failure, Comparison of Mercury and Water Data.....	54

INITIAL PHASES OF DAMAGE TO TEST SPECIMENS IN A CAVITATING VENTURI AS AFFECTED BY FLUID AND MATERIAL PROPERTIES AND CAVITATION REGIME

I. INTRODUCTION

The cavitation damage investigation being conducted in the authors' laboratory, and some of the preliminary results, have been described in previous papers[1,2] and project reports.[3,4] In brief, cavitation is produced in a venturi test section (Figure 1) located in either of two closed-loop tunnel facilities (Figures 2 and 3). Damage is observed on two (or three) test specimens (Figures 4 and 1), which project into the diffuser section. One surface (indicated in Figure 4) is metallographically polished and monitored for pitting.

The damage produced so far in these facilities is generally in its relatively initial phases in that it consists largely of individual small (order of mils diameter and from hundreths to tenths of mils depth) pits or craters which have not yet overlapped. While in some cases somewhat more severe damage has been observed, it is still not of the extensive type* sometimes observed in the field after long service. Nevertheless, it is felt that a study of these initial phases of damage will lead to an improved understanding of the later phases of damage.

The test specimens utilized are thin, tapered sections oriented parallel to the flow, and projecting away from the wall about 2/3 of the venturi radius at that axial location (Figure 1).

*On some of the longer run mercury specimens damage has been obtained which appears very similar to that noted on the interior passages of the centrifugal pump used in the loop after about 600 hours of cavitation.[4,1]

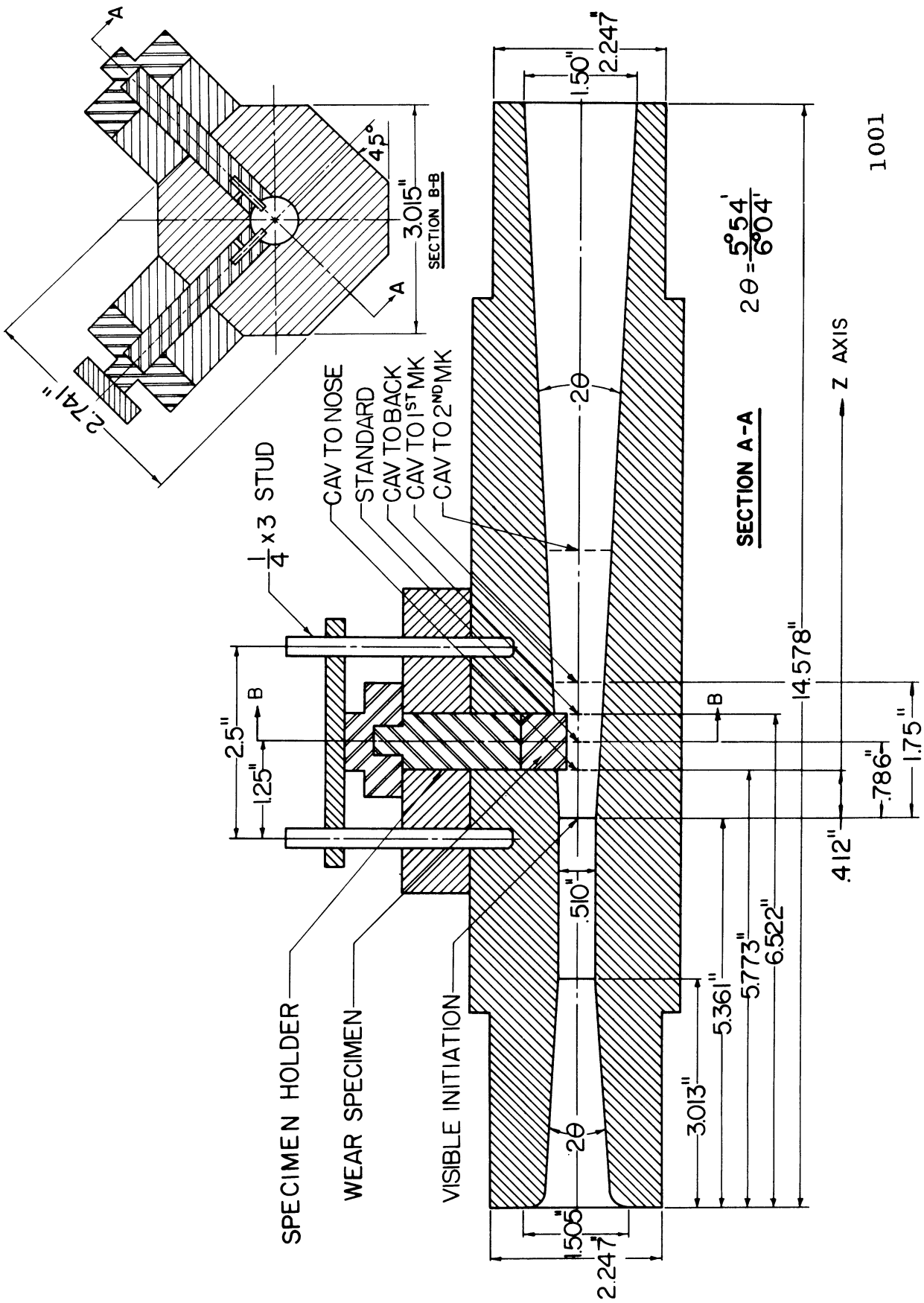

Figure 1. Drawing of the Damage Test Venturi Showing Location of Specimens, Specimen Holders and Cavitation Termination Points.

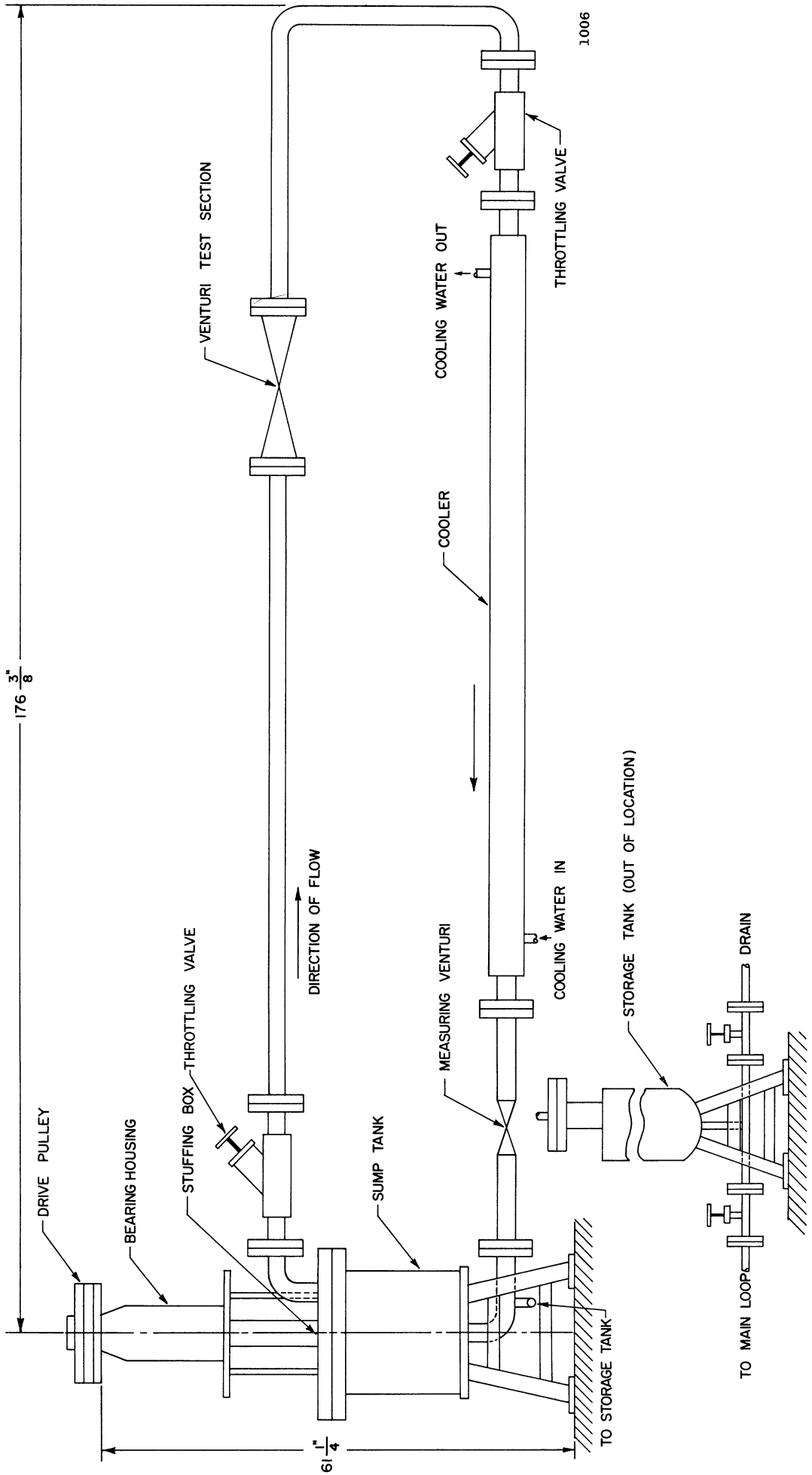

Figure 2. Schematic Drawing of Overall Mercury Loop Layout.

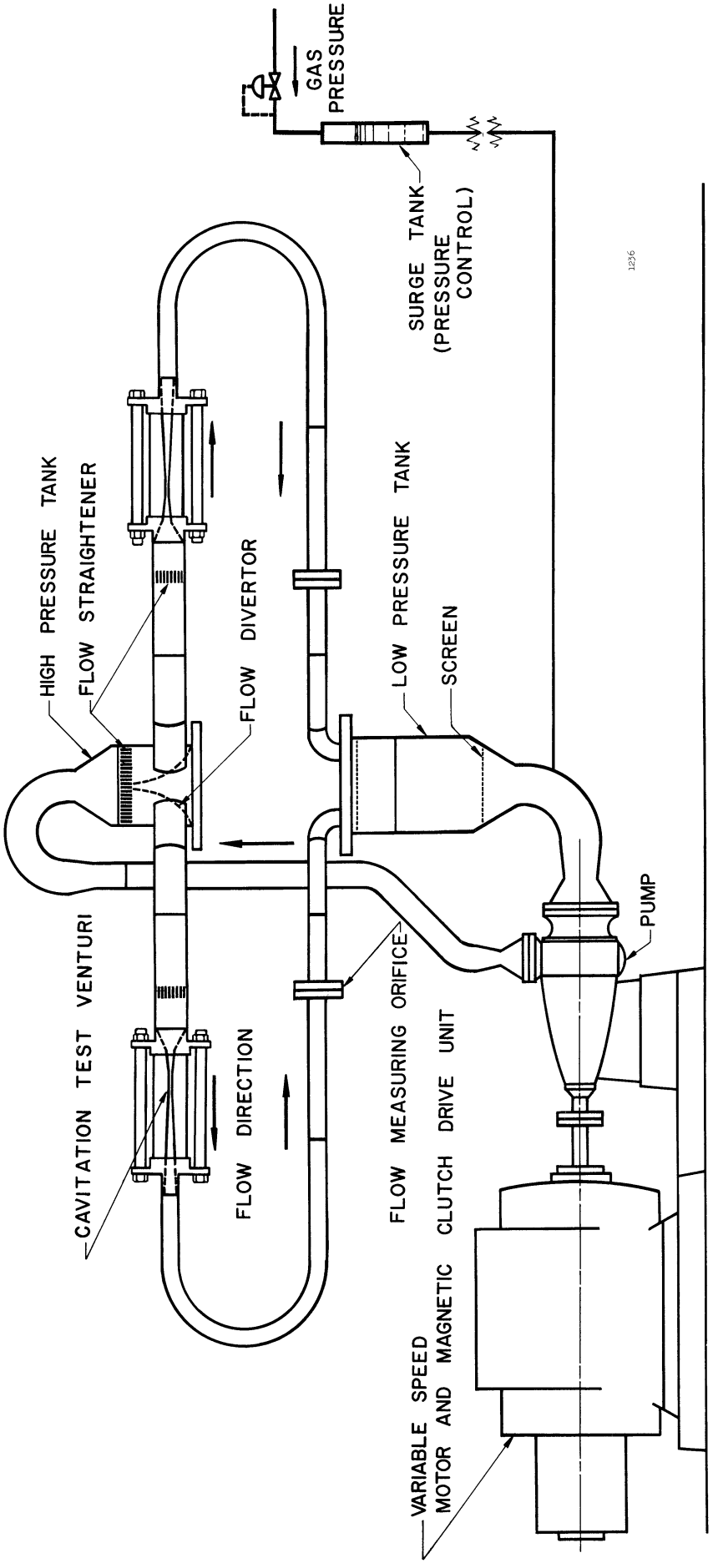

Figure 3. Schematic Drawing of Overall Water Loop Layout.

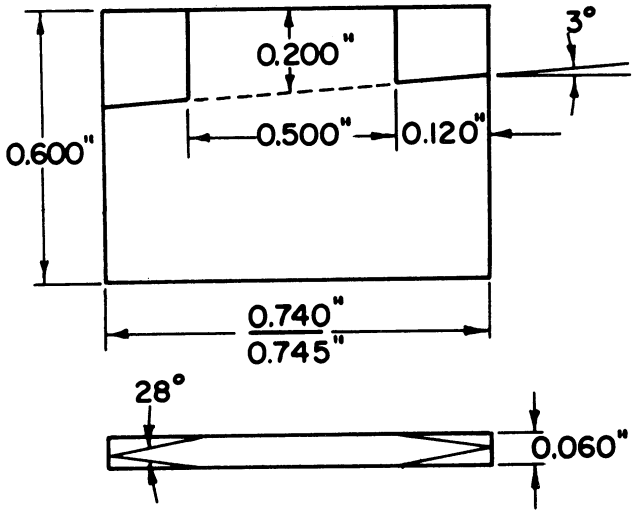

Figure 4(A). Drawing of Test Specimen.

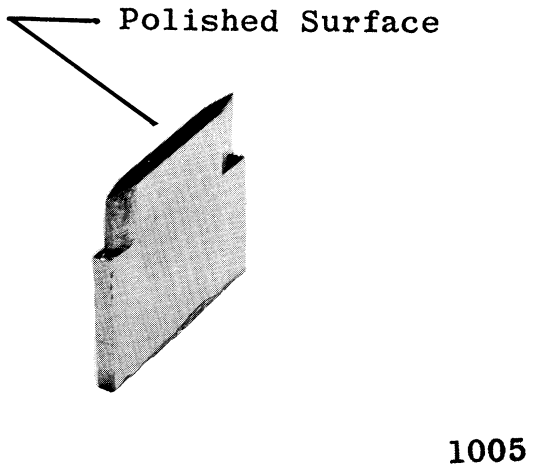

Figure 4(B). Photograph of Test Specimen.

By suitable adjustment of the flow-rate and pressures the cavitating region can be caused to terminate visually upstream, upon, or downstream of the test specimens. An arbitrary selection of "degrees of cavitation" has been made according to the apparent termination point. These conditions are listed in the appendix. As the degree of cavitation is adjusted from "Visible Initiation" toward more fully developed conditions, the positive pressure gradient, associated with the cavitation termination region, shifts downstream as indicated in Figure 5, so that the static pressures in the vicinity of the test specimens depend on degree of cavitation and flow-rate (velocity), with the higher pressures being associated with the lesser degrees of cavitation.

Previous papers[1,2] concerning this investigation have discussed some of the characteristics of the pits which are formed and the probable mechanism involved, and hve presented some preliminary quantitative data on the volume removed by cavitation from the test specimens.

The present paper examines and discusses the effects upon the pitting characteristics of cavitating flow regime, fluid properties (mercury and water), and material properties. In addition further quantitative damage data from tests wherein the above parameters were varied over substantial ranges is presented. From this data normalized mean depth of penetration* is plotted against the various material mechanical properties in an attempt to show possible correlations.

---

*"Mean depth of penetration" can also be thought of as "specific volume loss", i.e. volume removed per unit area exposed.

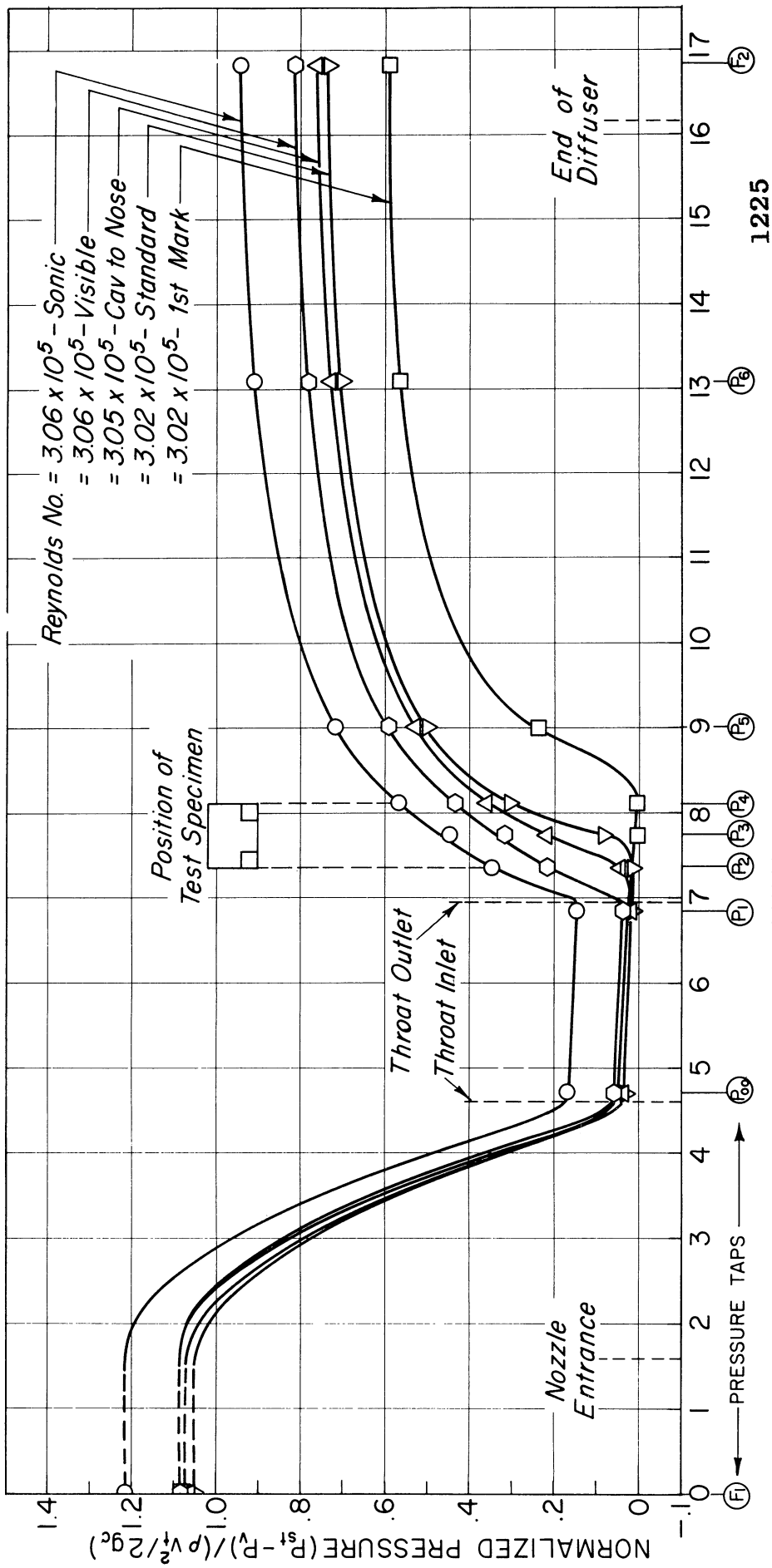

Figure 5. Normalized Axial Pressure Profiles for Several Cavitation Conditions with Water (1/2 inch venturi test section No. II).

II. PITTING CHARACTERISTICS AS AFFECTED BY FLOW, FLUID AND MATERIAL PARAMETERS

A. Degree of Cavitation Effects

Figures 6 through 11 are composite photomicrographs of the initially polished surfaces of five stainless steel* test specimens after exposure to cavitation in mercury at 34 feet/second throat velocity under the cavitation conditions (as defined in the Appendix) of:

i) Visible Initiation

ii) Cavitation to Nose

iii) Standard Cavitation

iv) Cavitation to Back

for various durations. An examination of these figures shows the following.

1. Pit Size and Number Density Distribution

As the degree of cavitation is increased from "Visible Initiation" (lowest degree producing substantial damage in mercury) through the intermediate conditions to "Cavitation to Back", the location of the damaged region tends to shift toward the rear of the specimen, as would be expected. Also the type of pitting varies throughout the damaged region. Toward the upstream end of the region the pits are very small and numerous; toward the downstream end they

*The applicable mechanical properties of all materials involved are listed in Table I.

TABLE I

Typical Mechanical Properties of Materials Tested

Material	Condition	Tensile Strength psi	0.2% Yield Strength psi	% Elong. in 2 in.	% Reduction in Area	Hardness		Bending Fatigue Strength psi	Elastic Modulus
						Measured Rockwell B	BHN		
Stainless Steel (300 Series)	Annealed	98,000	37,000	55	65	76	140*	35,000 @ 10^7 cycles	28 x 10^6
1010 Carbon Steel	Annealed	50,000	30,000	40	71	48	85*	25,000 @ 10^7 cycles	28 x 10^6
Aluminum 1100-0(2S0)	Annealed	13,000	5,000	35	-	-	23**	5,500 @ 10^7 cycles	10 x 10^6
Aluminum 6061-T6(61-ST6)	Age Hardened	45,000	40,000	12	-	57	90*	13,500 @ 10^7 cycles	10 x 10^6
Plexiglass	-	10,445*	-	2-7	-	-	M90-M100 Rockwell**	-	0.4 x 10^6*
Cb-1Zr	20% Cold-Worked	56,000	52,500	6	84	-	-	—	—
Stainless Steel (410)	-	95,000	78,000	22	-	-	185**	-	29 x 10^6
Aluminum AMS-4220 T-77	-	30,500	23,000	2.0	-	-	75**	-	10 x 10^6
Stellite	-	--	--	-	-	-	341	-	--

* Measured value or converted from measured value.

** Typical value.

become considerably larger and not as numerous. This is particularly true of the small crater-type pits of which there are very many on these specimens, and which are presumably caused by the implosion of single bubbles.* In the middle region of the damaged area the orater-type pits reach a maximum number density, and cover the complete size spectrum.

The distributions of pit size and number density is believed to result from the fact that bubbles are most numerous in the upstream portions of the damaged area but, because of the low static pressure in these regions (Figure 5), have a minimum driving force for collapse. In the downstream regions of the damaged area the static pressure is considerably greater because of the action of the diffusing portion of the venturi downstream of substantial two-phase flow (Figure 5). Hence the driving force for collapse in this region is much greater. There is a more violent collapse of these few bubbles which penetrate into the region of higher pressure, so that generally fewer but larger pits of the single-bubble crater type are produced. For "Cavitation to Back" (Figure 9) there is no region of large pits, i.e. the region of higher static pressure is downstream of the specimens entirely.

2. Detailed Flow Effects

Although the previous comments have been concerned with the axial distribution of pitting, an examination of any of the composite photomicrographs (Figures 6-11) shows that the distribution also is not uniform in the circumferential direction. The pattern is in the

*This presumption is based on strong circumstantial evidence which indicates that all pits, symmetrical or otherwise, are single event failures, but, because of their symmetry, the crater-type are also single blow events.

The local distribution of the larger, irregularly-shaped pits presumed due to many blows is believed more a function of inclusions or other surface defects than of fluid-dynamic parameters.

form of a wake, originating along one side of the specimens. This can be seen particularly well in Figure 11, which shows the two specimens tested together in the venturi at "Visible Initiation" after 10 hours duration. As installed in the venturi (Figure 1), the test specimens are separated by an angle of 90°, leaving a complimentary angle of 270°.* In Figure 11, the specimens are oriented as they would appear to an observer opposite the smaller (90°) opening. It is seen that the wakes originate from the flow through the narrower opening, indicating that the relative flow to the test specimens has a cross-wise component in the direction of the wakes, away from the more restricted region of the 90° separation, and generating bubbles as it encounters the sharp lengthwise edge of the test specimens.

3. Quantity of Pitting

The quantity of pitting of course increases with test duration as is particularly evident from an examination of Figures 6, 7, 10, and 11, where the development of pitting for "Visible Initiation" and "Cavitation to Nose" can be compared for various durations up to 25 hours. Precise quantitative results from weight measurements, showing the effects of duration and degree of cavitation, will be discussed in a later section. However, for the moment it is noted that the damage resulting from these two degrees of cavitation is quite similar. It is believed that in both cases the damage is caused mainly by bubbles generated in local cavitation from the test specimens themselves,

*Venturis with three equally spaced specimens have been used in the more recent water tests.

and that the main influence of the increase of degree of cavitation in this range is simply a reduction in the local static pressure affecting the local cavitation.

B. Fluid Effects

1. Type of Pitting

Some information on the effects of fluid parameters, when they are varied over a very wide range, on pitting characteristics is afforded by a comparison of the water and mercury results. Since, for the test materials used, corrosion was not significant in either fluid, it is believed that the differences noted are mainly due to the large density and vapor pressure differences between the fluids (all tests are at room temperature).

Figure 12 is a composite photomicrograph of two stainless steel specimens exposed to "Standard Cavitation" in water, at a throat velocity of 65 feet/second, for a duration of 191 hours. The mean depth of penetration is estimated to be about equal that of the specimen tested in mercury under the same cavitation condition for a duration of 10 hours (Figure 8). As will be noted, the damage on the water specimen is composed predominently of relatively large pits of irregular outer contours, presumably the result of fatigue failures due to repeated (relatively weak) blows, rather than the smaller, apparently single-blow, crater-type pits encountered on the mercury specimens. This apparent predominence of more powerful blows in the mercury test would of course be expected both from the density and vapor pressure (less cushioning effect) differences.

2. Shape, Size, and Spatial Distribution of Pits

Detailed pit tabulations have been made on a pair of stainless steel specimens exposed to 100 hours of "Visible Initiation" cavitation in mercury at 34 feet/second throat velocity. These are presented in Table II and can be compared with similar observations from stainless steel specimens cavitated (at various degrees of cavitation and durations) in water at 65 feet/second throat velocity presented in Table III (reproduced from reference 1 for convience). Comparison shows that in all sizes the proportion of approximately symmetrical (i.e. crater-type) pits in the mercury tests is greater (order of 25-30%) than that in the water tests. The tabulated proportion of craters is of the order of 15% but it is believed that the actual proportion is greater because it is likely that many of the somewhat irregular pits, especially in the smaller sizes, are also the result of single blows. Thus the trend noted in the previously discussed photomicrographs is somewhat substantiated by these observations.

The proportion of the total number of pits found in each size category is shown in Table IV (exclusive of the "small" category which was not counted in the mercury tests). It is noted that the water specimens have a larger proportion than do the mercury specimens in the larger size categories. Assuming that the larger pits are generally of the multi-blow fatigue type, this is consistent with the previous observations.

TABLE II

Comparison of Sizes and Percent Circular Pits On Mercury Samples

TABLE II-A % Circular Pits of Total

Sample No.	Sample Position	Cavitation Condition	Velocity (fps)	Duration (hrs.)	Observed Area	Pit Size Categories (mils) VVL 5.52 ≤ Dp < 11.04 % Cir.	VVL Total	VL 2.76 ≤ Dp < 5.52 % Cir.	VL Total	L 1.15 ≤ Dp < 2.76 % Cir.	L Total	S 0.46 ≤ Dp < 1.15 % Cir.	S Total
64-3	Front	Nose	34.8	100	Polished Surface	7.7	26	13.8	29	12.8	94	--	
					Numbered Side	16.1	31	18.75	32	25	200	--	
					Opposite Side	8.9	45	25.7	39	16.9	130	--	
					Sub-Total (Both Sides)	11.8	76	22.6	71	21.8	330	--	
					Sub-Total (All Surfaces)	10.8	102	20	100	19.8	424	--	
63-3	Back	Nose	34.8	100	Polished Surface	7.4	27	16.1	31	19.2	73	--	
					Numbered Side	13.33	15	15.0	40	15.3	150	--	
					Opposite Side	10.0	20	22.2	45	18.2	110	--	
					Sub-Total (Both Sides)	11.4	35	18.8	85	16.5	260	--	
					Sub-Total (All Surfaces)	9.7	62	18.1	116	17.1	333	--	
					Total (64-3 & 63-3)	10.4	164	19.0	216	18.6	757	--	
					% of Total (exclusive of small)		14.4		19.0		66.6		

TABLE II-B Total Pits Per In^2 HR.

Sample No.	Sample Position	Cavitation Condition	Velocity (fps)	Duration (hrs.)	Observed Area	VVL Pol.	VVL Sides	VL Pol.	VL Sides	L Pol.	L Sides	S Pol.	S Sides
64-3	Front	Nose	34.8	100	----	7.0	2.54	7.8	2.38	25.3	11.05	--	
63-3	Back	Nose	34.8	100	----	7.3	1.17	8.3	2.84	19.6	8.7	--	

Where: Pol = Polished Surface and Sides = Total for Both Sides

TABLE III

PIT COUNT TABULATIONS*

Pit Count and Various Sizes

		Pit Size (mils)							
		VVL		VL		L		S	
		(10 > D > 5)		(5 > D > 2-1/2)		(2-1/2 > D > 1)		(1 > D > .4)	
		% Cir.	Total	% Cir.	Total	% Cir.	Total	% Cir.	Total
Sample No. 4-3	Polished Surface	10.0	10	23.4	17	17.33	75	12.5	400
Sample Position.....Front	Numbered Side	21.75	23	18.7	48	16.05	81	15.1	325
Standard Cavitation	Opposite Side	18.75	16	21.1	19	14.55	55	4.9	465
Throat Velocity.....64.5fps	Subtotal (2 sides)	20.5	39	19.4	67	15.45	136	9.1	790
Duration of Run.....150 hrs.	Total All Surfaces	18.4	49	21.4	84	16.1	211	10.3	1190
Sample No. 5-3	Polished Surface	15.4	13	22.2	18	25.4	110	25.8	480
Sample Position.....Back	Numbered Side	11.1	9	21.1	19	15.9	63	16.3	320
Standard Cavitation	Opposite Side	6.3	32	7.2	14	10.2	49	12.9	350
Throat Velocity.....64.5fps	Subtotal (2 sides)	7.4	41	15.2	33	13.4	112	14.5	670
Duration of Run.....150 hrs.	Total All Surfaces	9.3	54	17.7	51	19.4	222	19.2	1150
Sample No. 18-3	Polished Surface	0	11	4.5	23	6.8	74	15.0	320
Sample Position.....Front	Numbered Side	0	29	5.0	40	5.9	51	13.5	200
Cavitation to Nose	Opposite Side	0	13	9.1	11	9.1	33	12.3	130
Throat Velocity.....64.5fps	Subtotal (2 sides)	0	42	5.9	51	7.2	84	13.1	330
Duration of Run.....50 hrs.	Total All Surfaces	0	53	5.4	74	7.0	158	14.0	650
Sample No. 19-3	Polished Surface	9.1	33	17.2	64	15.0	100	10.2	365
Sample Position.....Back	Numbered Side	5.3	19	0	14	9.3	43	18.7	150
Cavitation to Nose	Opposite Side	11.1	9	0	16	7.7	26	8.6	105
Throat Velocity.....64.5fps	Subtotal (2 sides)	7.1	28	0	30	8.7	69	14.5	255
Duration of Run.....50 hrs.	Total All Surfaces	8.2	61	11.7	94	12.4	169	11.9	620
TOTAL ALL 4 SAMPLES		8.75	217	13.9	303	14.3	760	14.1	3610

TABLE IV

Comparative Size Distribution of Pits

Percent of Total Pits (Exclusive of "Small") in Category

	VVL	VL	L
Mercury	14.4	19.0	66.6
Water	17.0	23.5	59.4

C. Test Material Effects

1. Effects of Grain Boundaries on Pitting Location

The stainless steel specimen shown in Figure 8, cavitated in mercury, was etched prior to testing to determine the existence of any possible relation between the grain boundaries and the location of pits and their shapes. As expected the crater-type pits seem to fall completely at random, their location not influenced by the grain configuration. Sometimes, however, the profiles of the irregular-shaped pits follow the grain boundaries for part of their contour, indicating that the location and shape of this type of pit is a function of the local surface material properties in addition to the flow parameters.

2. Effect of Surface Finish

To investigate the effect of surface finish, two sets of stainless steel specimens were prepared for mercury tests; one set was polished on all wetted surfaces ($\sim$ 2.0 microinch rms), and the other remained in the machined condition (20 to 25 microinch rms) on all wetted surfaces. Each set was tested for 50 hours duration at "Standard Cavitation" with 34 feet/second throat velocity. The results, listed in Table V, are somewhat surprising in that the completely unpolished specimens showed the smallest weight loss, the completely polished specimens the highest, and a set of regularly prepared specimens (polished only on the usual "polished surface", which is about 1/9 the wetted surface) tested under the same conditions, was intermediate. While the spread in volume loss is substantial (about 50% in the extreme case), it is not necessarily beyond the possible scatter due to inhomogeneity of material, dimensional differences between specimens, minor flow differences, etc.

TABLE V

Data On Surface Finish As A Cavitation Damage Parameter

Test Conditions:

Standard Cavitation
2.5" Flow Rate (34 fps.)
Stainless Steel Samples

Sample Condition	Total Weight Loss For 2 Samples (mg.)	Ratio To Unpolished
Regular (47 & 48)	4.27	1.20 : 1
Polished Sides (78 & 112)	5.46	1.53 : 1
Unpolished (81 & 82)	3.56	1 : 1
Rolled ⊥ To Flow (11-120, 12-120)	4.85	1.36 : 1

Note:

A. Surface finish of sides of regular samples (47 & 48) is between 20 - 25 μ in. (rms).

B. Surface finish of polished surface of regular samples is about 2 μ in. (rms).

C. Surface finish on 78 & 112 was about 2 μ in. (rms) on both sides and polished surface.

D. Surface finish on 81 & 82 was about 35 μ in. (rms) on "unpolished" surface and about 20 - 25 μ in. (rms) on sides.

E. Surface finish on 11-120 & 12-120 was similar to regular samples (i.e., 47 & 48).

It thus appears that the metallographic finish given the monitored surfaces of the test specimens in these tests does not significantly protect them from cavitation damage; in fact the available evidence shows the opposite. However, the machine finish used is extremely smooth compared e.g. with an ordinary cast pump impeller, so that no conclusions on the effect of rough surfaces upon cavitation damage can be drawn from the present tests.

3. Effect of Direction of Rolling

In some of the tests, it was noted that the damage often took the form of pits elongated in the direction of flow, i.e. parallel to the long direction of the test specimens (Figure 13) which, in the ordinary specimens, was also the direction of rolling. Hence it was suspected that these pits might represent the removal of inclusions, which had been squeezed by rolling to the elongated profile of the pits. To check this supposition, a set of stainless steel specimens was fabricated in such a manner that the direction of rolling was normal to the polished surface, i.e. normal to the direction of flow. These were tested for 50 hours duration under the same conditions used for the polished and unpolished specimen tests described in the last section. The results are also listed in Table V. The volume loss was somewhat increased (13.6%) over the standard test. This relatively small change is not necessarily beyond data scatter so that it cannot be concluded that the direction of rolling has any significant effect upon volume loss. No profusion of elongated pits was produced.

Figure 13. Cavitated Surface of Sample Number 55-3 Showing Elongated Pits in the Direction of Flow, Duration 1 Hour, Mag. 120X.

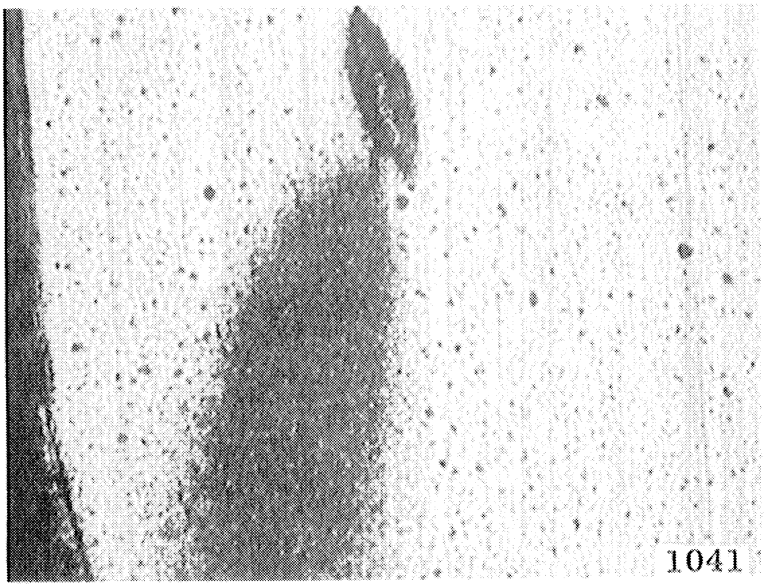

Figure 14. Cavitation Pit in Columbium-1% Zirconium After 40 Hours Exposure Showing Wake Formation.

4. Specific Material Effects

a. Carbon Steel Tests in Mercury

It was shown in a previous paper[1] that the general form of pitting encountered with water on carbon steel was similar to that observed on stainless steel, providing the test was short enough so that corrosive effects did not become significant. The present tests show that the same is true with mercury, although corrosion is not so significantly involved.

However, the damage rate of carbon steel with either fluid is considerably greater than that of stainless steel, so that in the case of the mercury tests,* where damage obtained in a given duration is of the order of 100 times that with water, effects of a new kind, as described below, have been observed with carbon steel.

In most tests conducted during the present investigation, it has been observed that the location of pits within the damaged region is essentially** random (within certain limitations as, for example, that larger pits form in regions of higher static pressure, etc.). However, in one extended carbon steel test it has been very clearly demonstrated that the previously incurred damage sometimes influences the location of subsequent attack. It is believed that in this case this is due almost entirely to a shifting of the cavitation region due to the change in surface

---

* A mercury venturi provides an intensified cavitation damage test in a flowing system, perhaps intermediate in degree of intensification between a water venturi and a water magnetostriction unit.

**Very large pits (Figure 14) sometimes form a wake influencing the distribution of subsequent pits. (Reprinted from refs. 1 and 4 for convenience.)

condition, rather than to any required incubation or preconditioning period for portions of the surface, since the demarcation between damaged and non-damaged regions is at all times extremely sharp, and even the single-blow crater-type pits are generally absent from an undamaged portion until the demarcation line has passed. This behavior is illustrated in a series of low-magnification photographs (Figures 15 - 17), showing two damaged carbon steel specimens, held between two unused specimens for comparison, after exposure to "Cavitation to Nose" in mercury at 34 feet/second for various durations, starting with 4 hours and proceeding to 77 hours.

In the first photograph (Figure 15), the orientation of the specimens has been inadvertently reversed, so that the adjacent sides correspond to the 270° separation in the venturi. It was previously shown (Figure 7) that the damage for this particular cavitation condition follows a wake pattern originating in the 90° gap, and angling across the specimens from this region. It is believed that this flow pattern results in the initial damage distribution, covering an area similar to that shown in Figure 7.

When the specimens were exposed to further cavitation the damaged area continued to spread in the upstream direction as indicated in the succeeding photographs (for which the orientation is correct). The wake pattern is still apparent, but the metal on the upstream side of the damaged region has

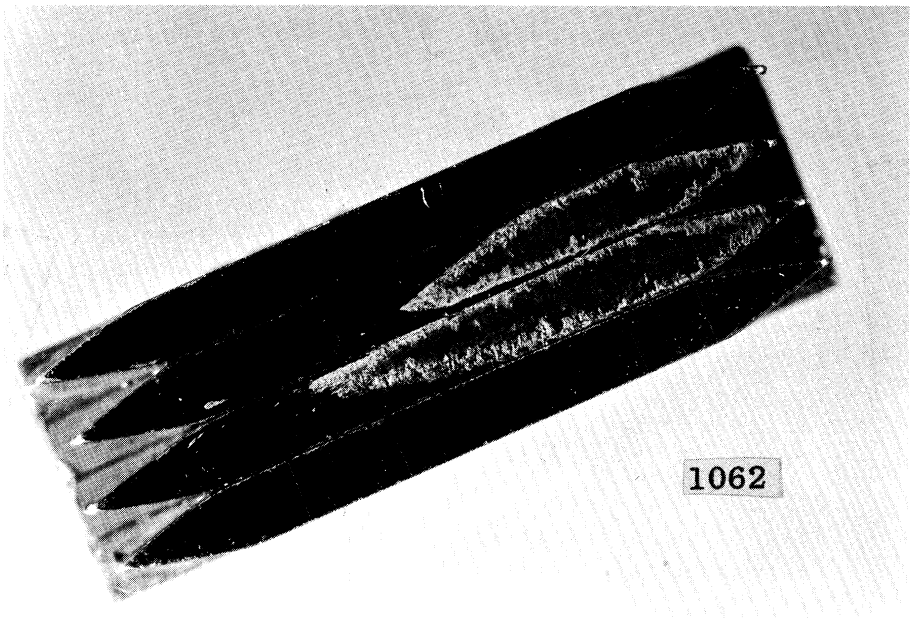

(a)

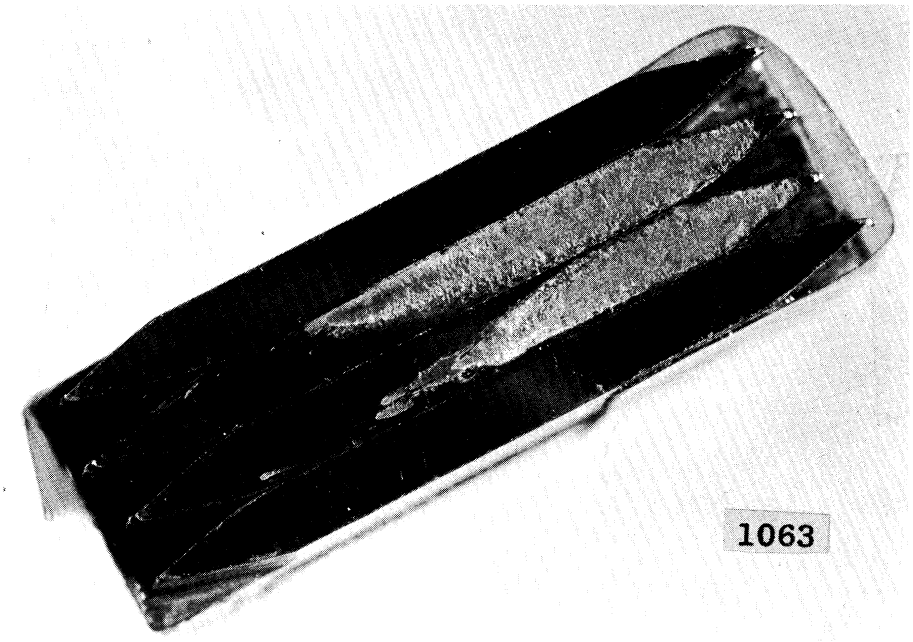

(b)

Figure 15. Macrograph of Cavitated Surface of Carbon Steel Samples Numbers 64-1 and 65-1 for "Nose" Cavitation Condition in Mercury at Throat Velocity of 34 feet/second. Outside Samples are Undamaged New Samples for Comparison. Mag. 4X. (a) 4 Hours (b) 7 Hours.

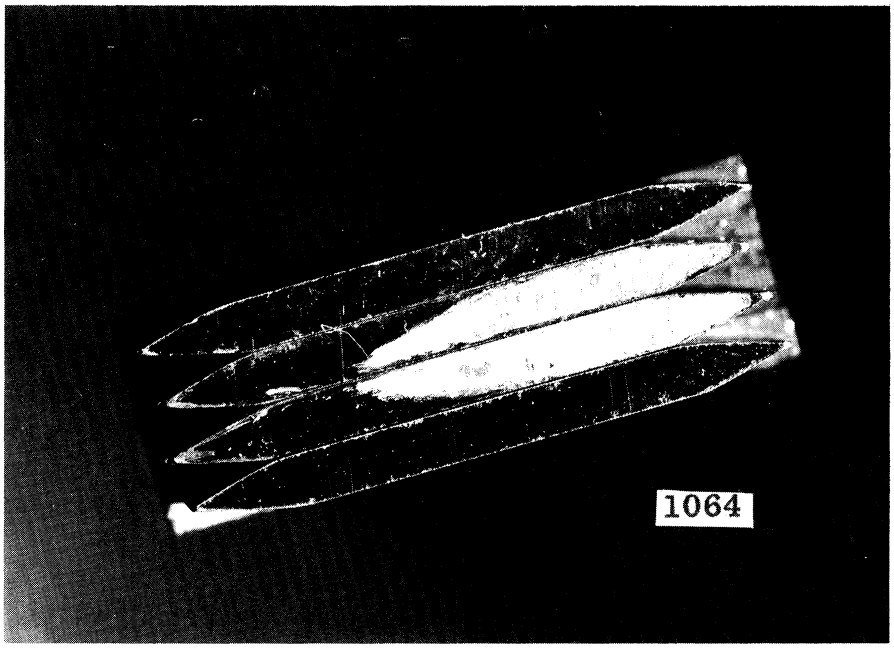

(a)

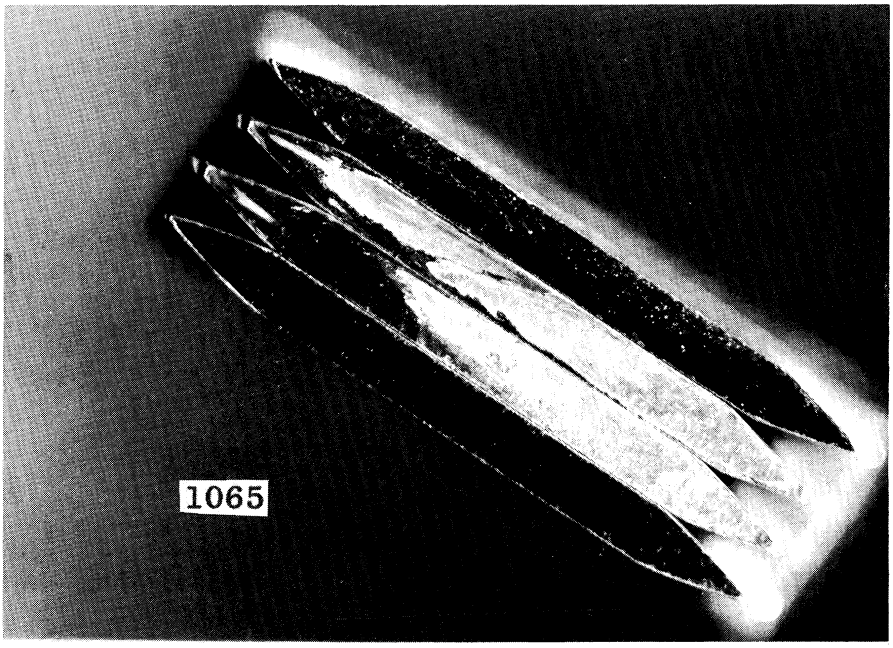

(b)

Figure 16. Same as Figure 52 except, (a) 17 hours duration, and (b) 37 hours duration.

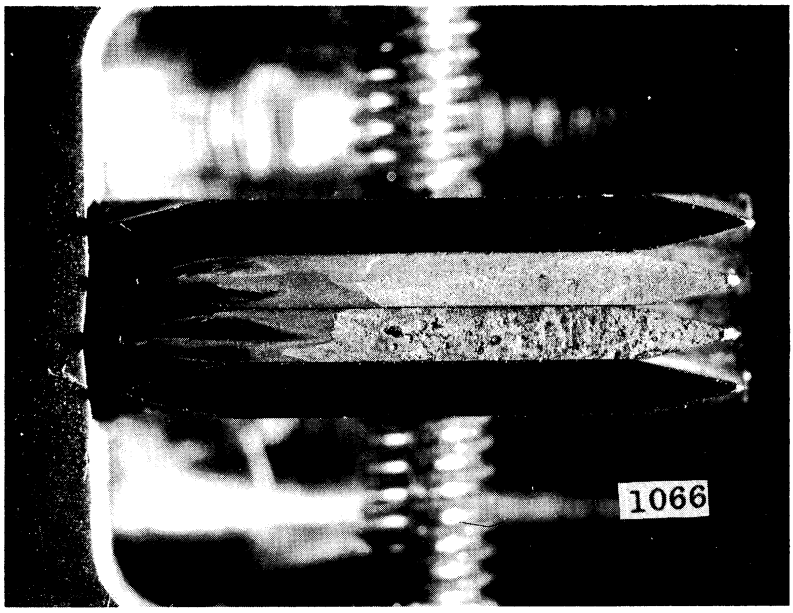

(a)

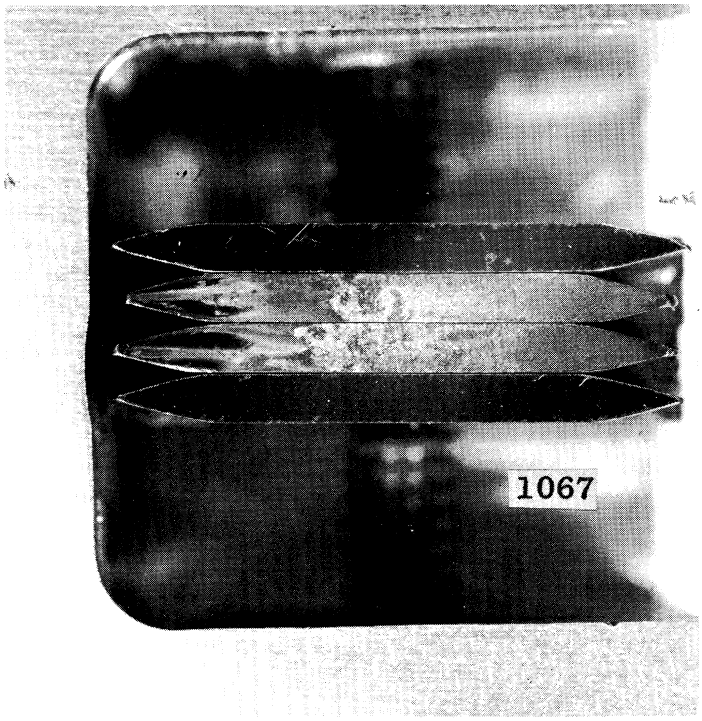

(b)

Figure 17. Same as Figure 52 except, (a) 77 hours duration, and (b) 100 hours duration.

now been attacked. However, the demarcation between damaged and undamaged areas is still extremely sharp, with the damaged portion having incurred several layers of pitting, while the undamaged region is essentially untouched. The region of the demarcation is shown with higher magnification and more detail in Figure 18.

This occurrance of a sharp damage cut-off, which advances into the undamaged material, is not unusual for heavily damaged specimens, having been previously observed e.g. in tests with a rotating disc apparatus.[5,6] Also somewhat similar behavior has been observed to a much lesser extent in the present tests with stainless steel (Figure 19).

b. Columbium-Zirconium Alloy Tests in Mercury

Damage of a sort not observed in the tests on the other materials has occurred in tests with mercury on Cb-1 Zr alloy,* in which there was an eventual** macroscopic fatigue-type failure, in which a thin surface layer covering an area of the order of 0.015 square inches peeled-off to a depth of about 2 to 3 mils (Figure 20). Figure 21 is a section through this region showing the continued propagation of cracks at the ends of the region. The microstructure of the material is shown in Figure 22.

*This type of failure is believed due to the cold-worked condition of the material, which would not be typical of high temperature applications.

**Prior to this the pitting was generally similar to that observed on the steels.

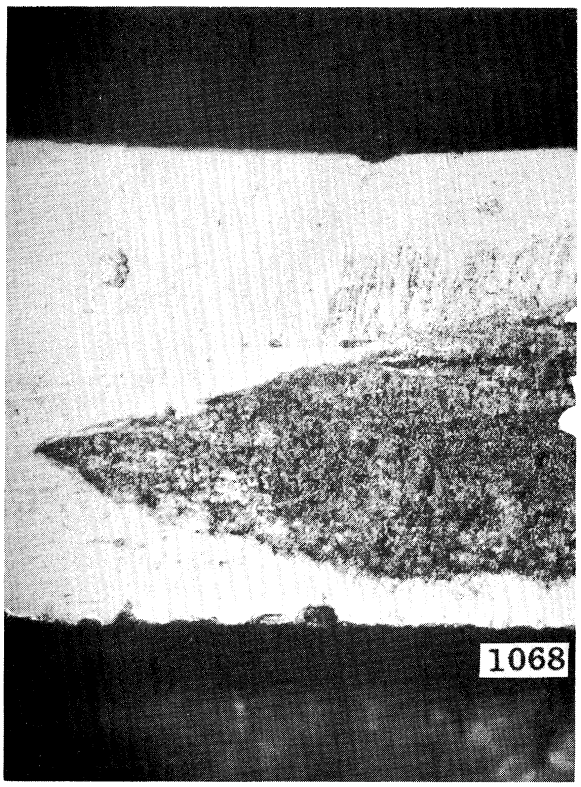

(a)

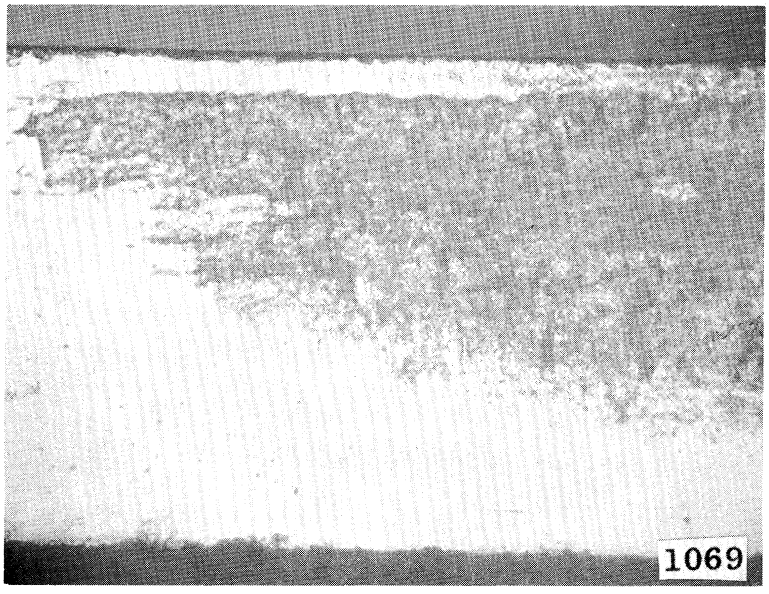

(b)

Figure 18. Magnified Picture of Damage Cut-off Region in Figure 52 (a). (a) Sample 64-1, and (b) Sample 65-1. Mag. 25X.

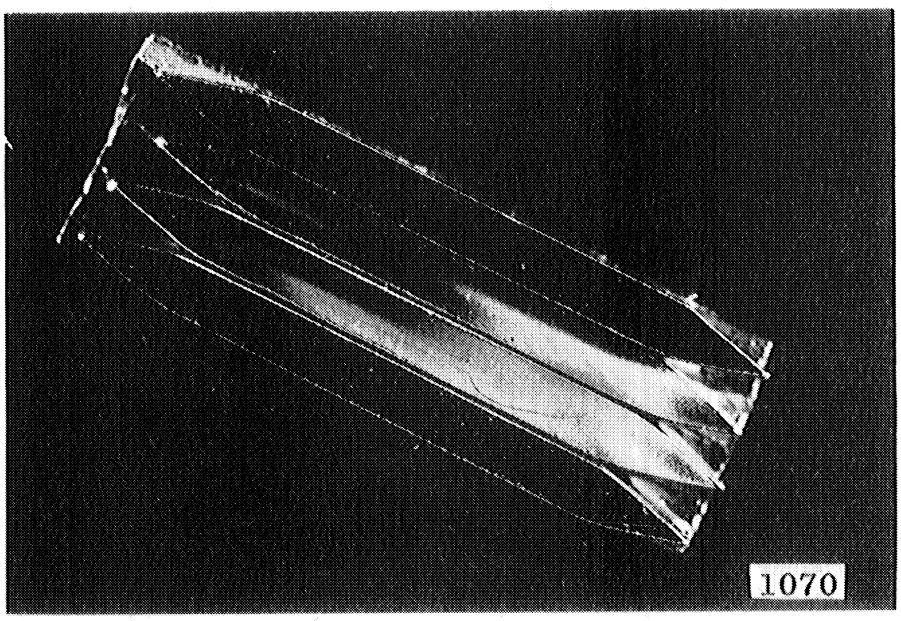

(a)

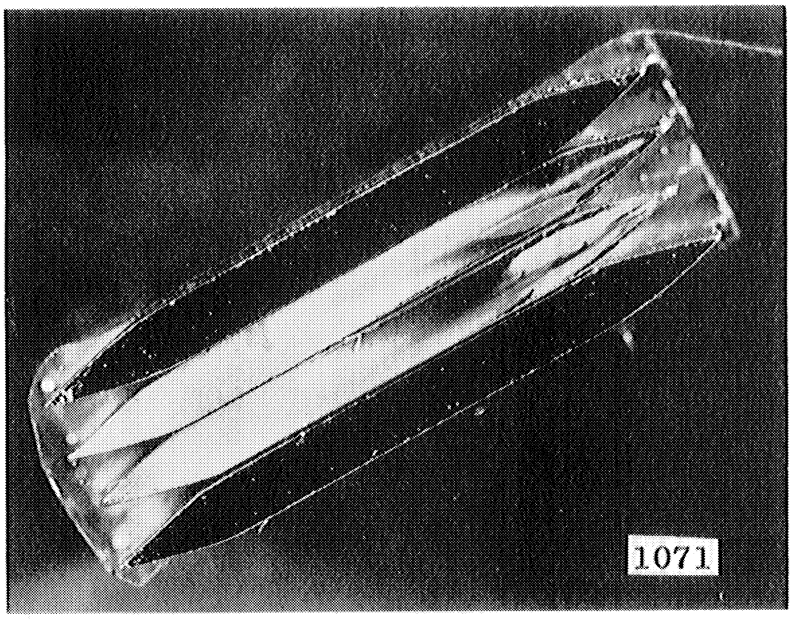

(b)

Figure 19. Macrograph of Cavitated Surface of Stainless Steel Samples Numbers 47-3 and 48-3 for "Standard" Cavitation Condition in Mercury at a Throat Velocity of 34 ft./sec. Undamaged Samples Included for Comparison. Mag. 4X. (a) 17 hours duration, and (b) 47 hours duration.

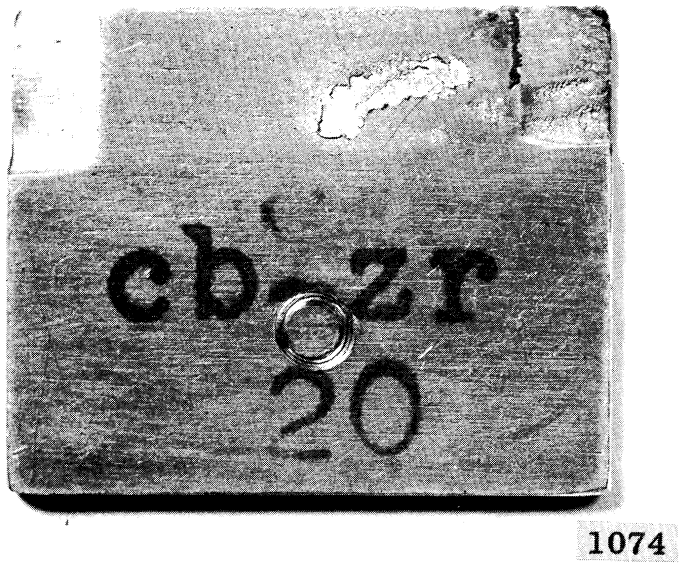

Figure 20. Macrograph of Numbered Side of Sample Number Cb-1Zr 20 After 50 Hours Exposure to "Nose" Cavitation Condition in Mercury at a Throat Velocity of 48 feet/second. Mag. 4X.

Figure 21. Microsection Through Gross Damage Area on Numbered Side of Sample Number Cb-1Zr 20 as Shown in Figure 58. Etched. Magnification 100X.

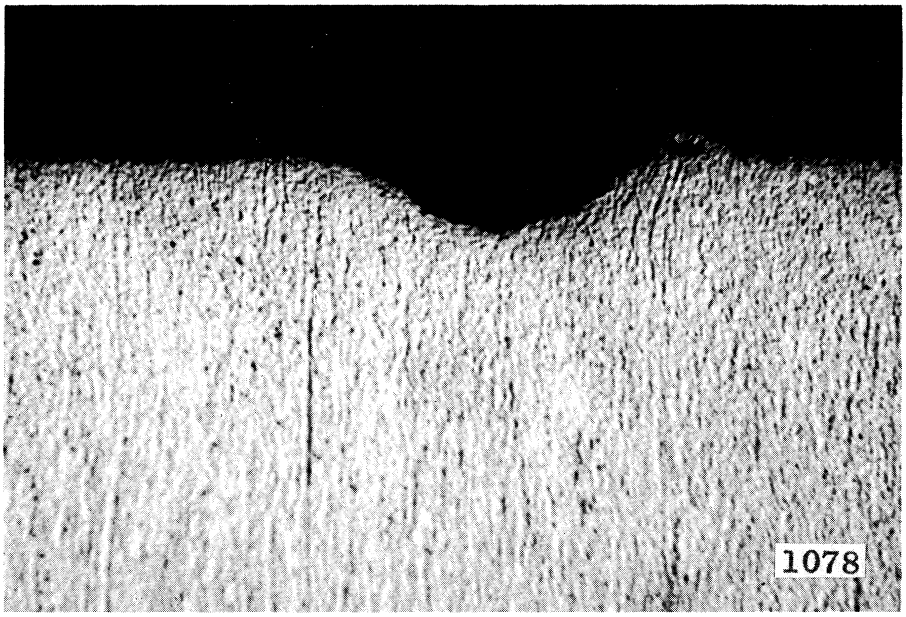

Figure 22. Microsection Through Cavitation Pit Labeled in Figure 68 After 50 Hours Exposure to Cavitation. Etched. Mag. 1000X.

III. QUANTITATIVE DAMAGE DATA

A great deal of quantitative damage data has been accumulated with both water and mercury (room temperature in both cases) as test fluids, and stainless steel, carbon steel, aluminum, various brasses, plexiglass, Cb-1 Zr, and other refractory alloys as test materials during the course of the present investigation;[3,4] and the work is still in progress. While it is not possible to report these results in detail in the present paper, the highlights will be summarized.

A. Degree of Cavitation Effects

The change of cavitation condition from initiation towards increased cavitation results in an increase in the number of bubbles in the vicinity of the test specimens, but a decrease in the collapsing pressure and hence energy of collapse. As might be expected under these conditions the damage goes through a maximum as the degree of cavitation is increased. With water this maximum occurs for "Visible Initiation"[1], whereas, for mercury it occurs for the increased condition of "Standard Cavitation". The preliminary results indicating the latter, previously published[1], have since been confirmed by much more comprehensive data (Figure 23). The reason for the differences between water and mercury in this regard is not presently known,* but the situation is indicative of the fact that the cavitation phenomenon does not in general scale according to the simple similarity laws.

*While the volume losses for water are calculated from pit counts and those for mercury from weight measurements, so that the absolute magnitudes are not entirely consistent, the data sets for each fluid should be internally consistent and hence can be used as indicated.

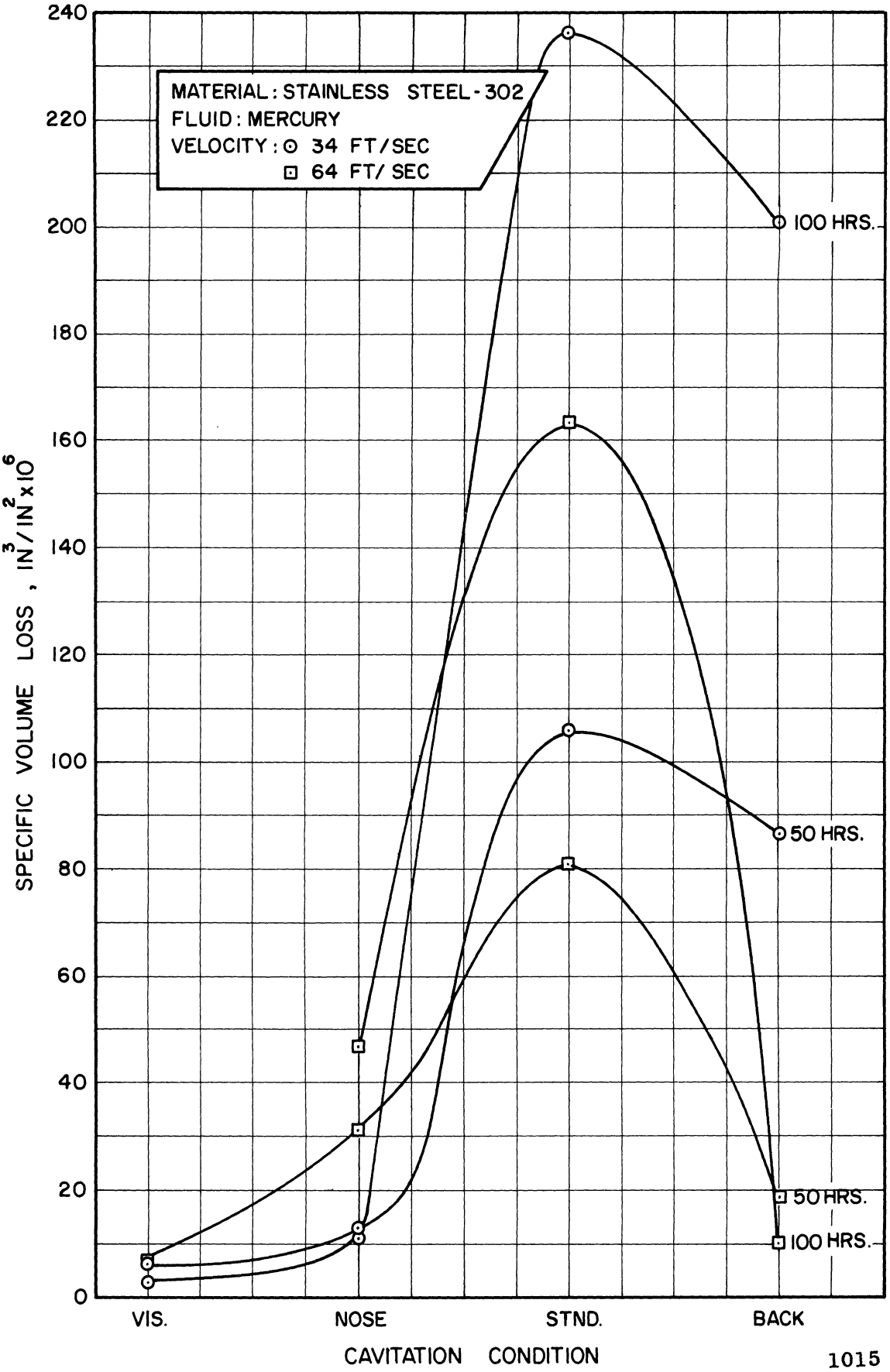

Figure 23. Actual Specific Volume Loss vs. Cavitation Condition for Constant Times for Stainless Steel in Mercury.

B. Throat Velocity

Previous investigations of velocity effects upon cavitation damage have generally shown that damage increases very rapidly with velocity, approximately proportional to the 6th power of the velocity.[7] Although no theoretical justification of such a relation is available, it has been roughly confirmed in several tests:

i) Rotating disc with through-holes as cavitation inducers.[5,6]

ii) Liquid jet impinging upon rotating test specimen[8]

iii) Cavitation upon an ogive in a water tunnel.[7]

However, the relations between the force-time loading on the surface and the volume removed, and again between the main stream velocity and the surface loading generated by collapsing bubbles is far from clear for any of the above devices, or for the venturi of the present tests. However, there is a basic difference between the present tests and those referenced above, in that in all the previous cases (but not in the present venturi) the geometry is such that the size of the damaged region changes with velocity. With the relatively small test specimens used in the present venturi this is not the case.

Velocity effects in the present tests have been generally much less* than previously reported.[5,6,7,8] In fact for well-developed cavitation the damage exhibits a maximum at an intermediate velocity and tends to decrease at higher velocity.** See Figure 24 for mercury tests on stainless steel wherein the velocity is varied over

*The velocity exponents for the present tests, positive or negative, generally lie between 1 and 2.

**An example of a decrease of damage with increased velocity is also reported for a rotating disc facility.[9]

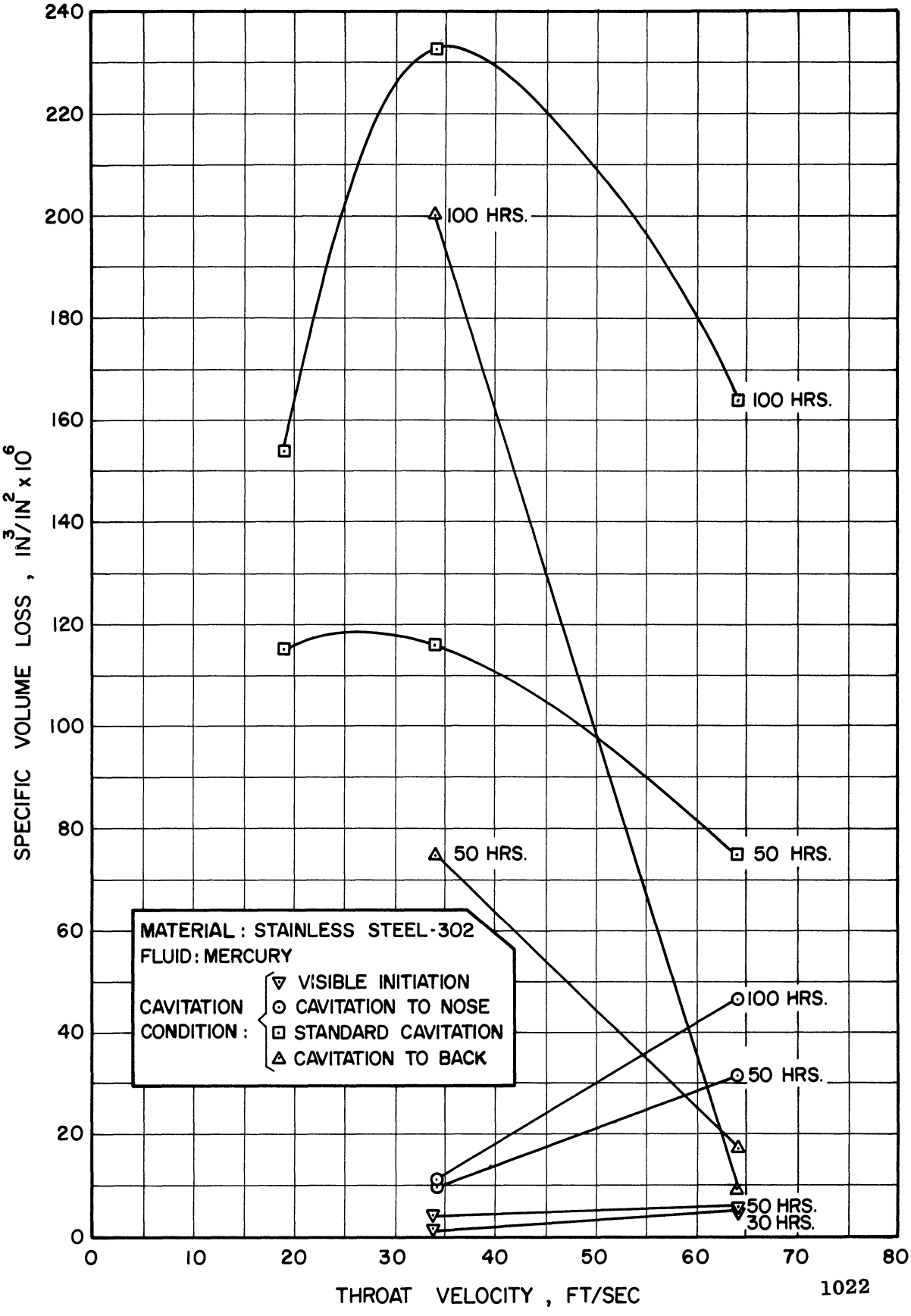

Figure 24. Actual Specific Volume Loss vs. Throat Velocity for Constant Time and Various Cavitation Conditions for Stainless Steel in Mercury.

about a 2:1 range for three degrees of cavitation. Damage decreases uniformly with velocity for the most developed cavitation ("Cavitation to Back"), shows a maximum at an intermediate velocity for "Standard Cavitation", and increases uniformly with velocity for "Cavitation to Nose." Similar behavior has also been observed with the other materials tested in mercury. So far the water tests are not sufficiently comprehensive for definite conclusions.

The dependence of velocity effect on degree of cavitation can be explained by the fact that the static pressure in the vicinity of the test specimens is a strong function of throat velocity for the initiation conditions (approaching the squared relation of single-phase flow), but does not vary substantially with throat velocity in the area of the test specimens for well-developed cavitation (i.e. two phase flow), remaining close to vapor pressure for all throat velocities. Thus the violence of collapse on the test specimens is not substantially a function of throat velocity for well-developed cavitation.

It appears that the above effect is coupled with another which somehow reduces either the number of bubbles in the critical region, i.e., adjacent to the test specimens, as the throat velocity is increased, or the static pressure in that region. In either case, further evidence of the lack of simple scaling of cavitating flow regimes is afforded.

C. Duration Effects*

Virtually all the curves of volume loss vs. test duration from the present investigation show, after an initial high damage rate,

*Op. Cit. footnote p. 12

a leveling-off period, followed eventually by a second period of high damage rate. The longest duration water-test curves presently available (Figure 25) are of this type.

In a sense, the mercury tests might be considered as accelerated (or intensified) water tests, in that for the same duration a much greater quantity of damage is incurred, so that it might be presumed that the behavior observed in mercury over a relatively moderate test time may illustrate the behavior to be expected in a much longer water test. If this is the case,** it is apparent that the relatively simple pattern so far observed in water will become more complex as duration is further increased. Figure 26 shows the presently available long-duration effects with mercury, at two throat velocities for stainless steel, and a single velocity for carbon steel. In all cases there was heavy pitting during the initial observation period, although in some cases the weight loss during this period was not large. Since the mercury curves become considerably more complex than those for water, it is not clear how best to extrapolate to longer durations.

D. Fluid and Material Effects

1. Fluid Effects

A direct comparison between the damage quantities attributable to mercury and water "other things being equal" is difficult because of the ambiguity of that condition, and the difficulty of achieving true similarity. For example, as previously discussed, the maximum

**It is obvious that it is not entirely the case, since these are differences in type of pitting between mercury and water, as previously discussed.

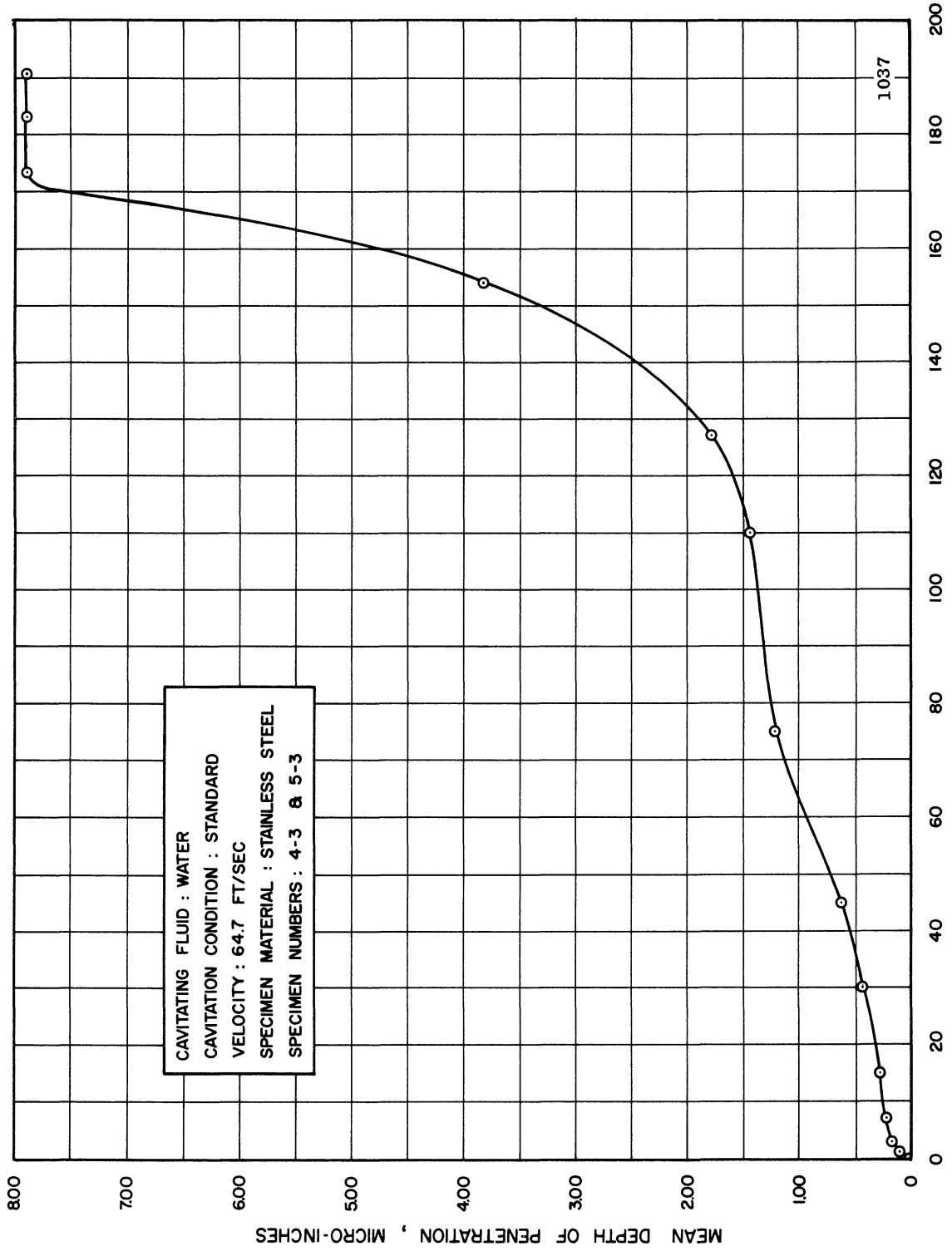

Figure 25. Mean Depth of Penetration vs. Time for Stainless Steel Cavitated in Water.

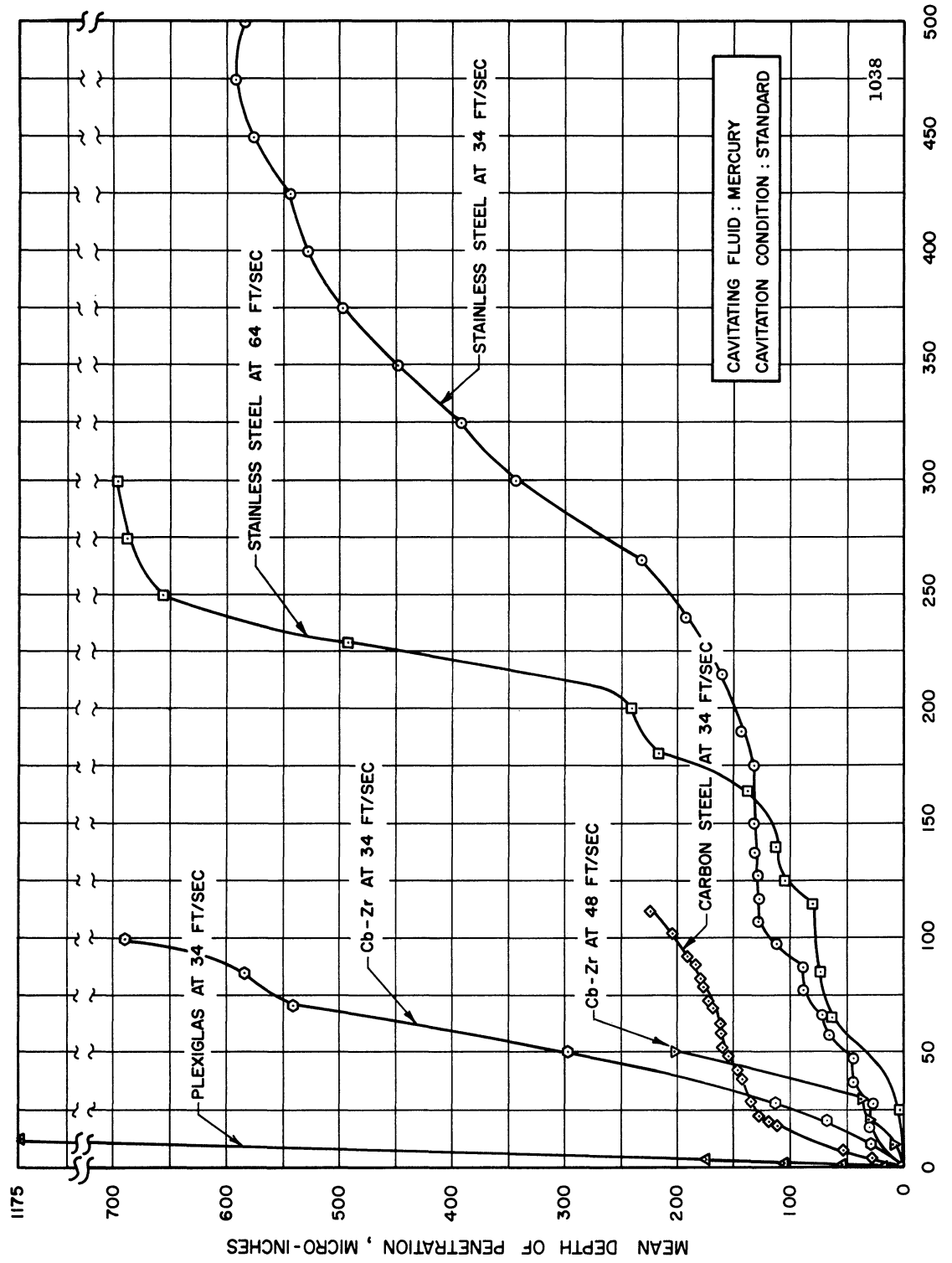

Figure 26. Mean Depth of Penetration vs. Time for Various Materials and Velocities in Mercury.

damage is obtained for different degrees of cavitation for the two fluids. However, rough comparisons have been made[4] between the maximum damage conditions. The making of such comparisons is further complicated by the fact that most of the quantitative damage results for water are based on calculation* from pit tabulations[4,10] (weight losses are usually insufficient for significant measurement), whereas those from mercury tests are based on direct weight measurement. The details of the estimating procedure are given in reference 4. For two sets of tests for which comparisons were possible the ratios of mercury to water damage were 47.5 and 135, giving a numerical average of 91. Hence a ratio of approximately 100 seems indicated.

2. Material Effects

In a previous paper[1] comparative data in water between aluminum, carbon steel, stainless steel, and plexiglas were given. The volume loss of the aluminum was very great compared to the steels; carbon steel showed about twice the volume loss of stainless steel in short tests before corrosion became significant; and plexiglas appeared to show less damage than stainless steel.**

Comparative results are shown for the mercury tests (Figures 27 and 28) between carbon steel, stainless steel, Cb-1 Zr, and plexiglas for two degrees of cavitation.*** It is believed that corrosion is not

*In spite of considerable care in measurements[10], the volume loss computed from pit counts was always considerably less than that derived from direct weight loss measurement. It is felt that a significant volume removal in the form of a thin uniform layer, by another mechanism other than the formation of discreet pits is involved.

**Based on pit-count data. Since pit observation on the transparant plexiglas was difficult, the quantitative data on plexiglas is uncertain. However, the over-all conclusion is confirmed by lack of pitting in the venturi walls themselves after very long exposure.

***Based on direct weight measurement.

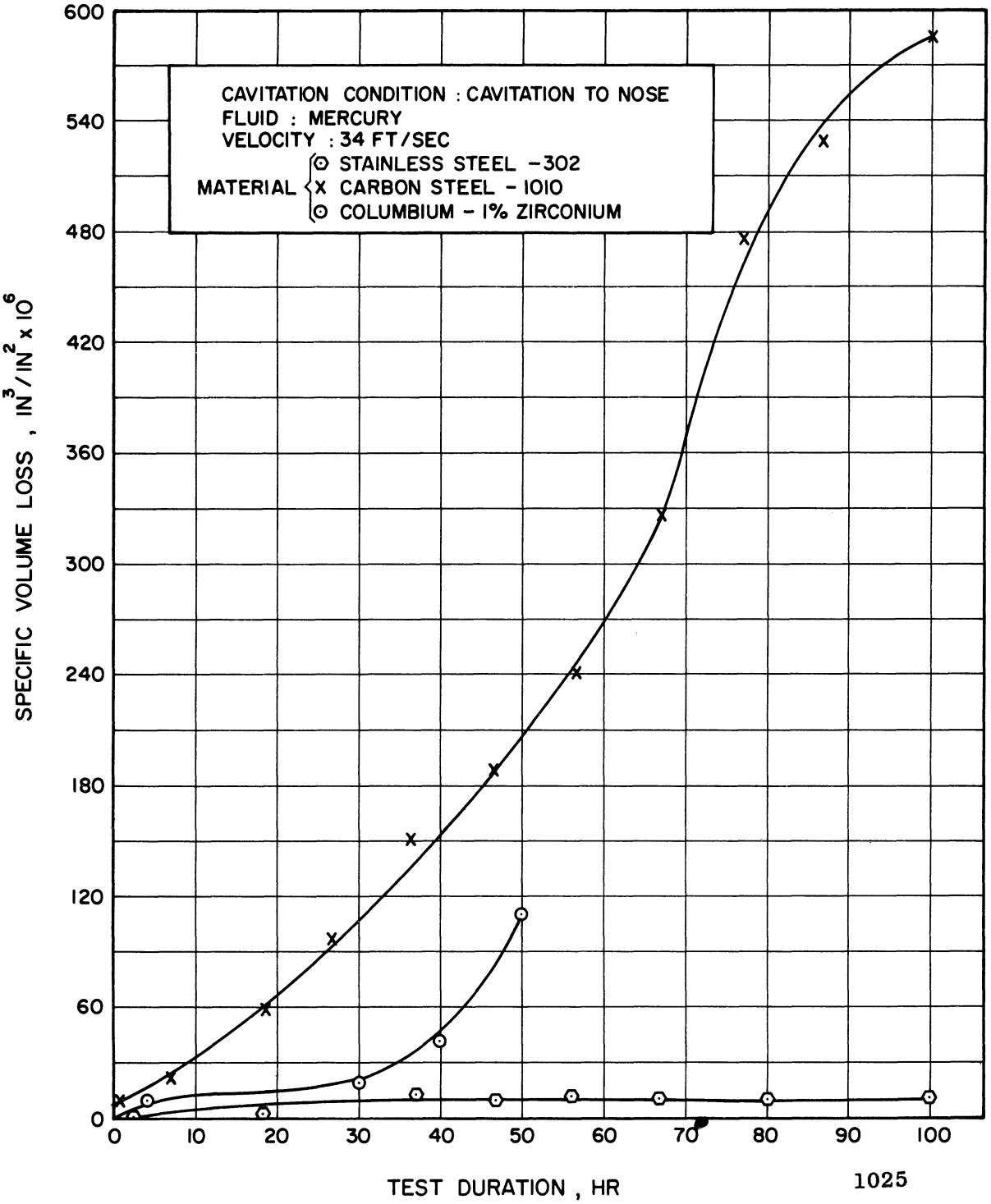

Figure 27. Actual Specific Volume Loss vs. Time for Different Sample Materials in Mercury.

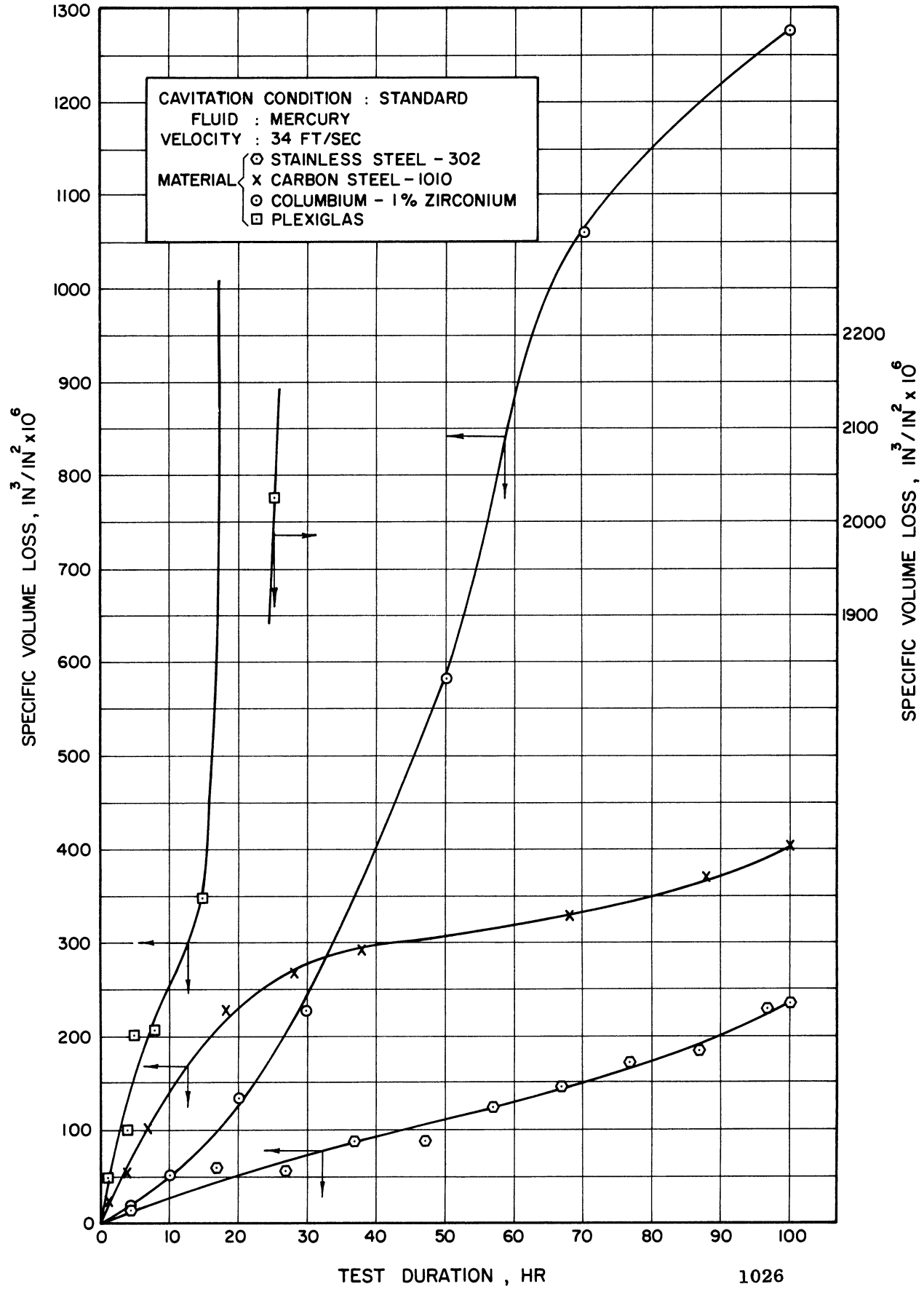

Figure 28. Actual Specific Volume Loss vs. Time for Different Sample Materials in Mercury.

important for any of these combinations. However, there is some dependence of relative resistance of the different materials on degree of cavitation, but for both cavitation conditions, stainless steel shows least damage and plexiglas most.

IV. CORRELATION WITH MATERIAL MECHANICAL PROPERTIES

A. Theoretical Considerations

An over-all objective of cavitation damage research is the determination of a grouping of material, fluid, and flow parameters which could be used to correlate cavitation damage in general, and thus allow the prediction of damage in advance. For the present this objective appears unattainable in the completely general case. However, under certain restricting assumptions, it may be possible to determine suitable correlating parameters.

In this connection it is usually assumed that:

i) consideration is to be limited to a single type of cavitating flow regime, and

ii) only mechanical damage effects are significant (or, alternatively, only chemical effects).

These assumptions may be applied to the present venturi tests, wherein the fluid-material combinations are such that corrosive effects are generally insignificant (except perhaps for the carbon steel in water combination).

It has been found by many previous investigators that increased tensile strength, surface hardness, yield strength, endurance limit, etc. will usually result in reduced cavitation damage, under the above assumptions, although there are usually numerous exceptions. More recently it has been emphasized that strain energy[11] may be of paramount importance.

It has been previously stated in connection with the present investigation that the pits appear to be either craters resulting from single-bubble implosions or fatigue-failures resulting from numerous blows, that the crater-type of pit becomes relatively more numerous for a high density fluid such as mercury, and that neither mechanism appears negligible.* It is believed that the parameter groupings which would correlate these two types of damage are different.

It seems likely that strain energy to failure may be of predominent importance in determining resistance to the formation of crater-type pits: however, resistance to conventional fatigue failure would certainly also involve the endurance limit.** A very large number of blows which did not create stresses in excess of the endurance limit would not cause failure or any permanent effect, even for a very brittle material.

In addition to the above, there are numerous other parameters and related effects which may require consideration. For example, there is the question of coupling between the relatively short range forces produced by a bubble implosion and the material surface with its ability to deform elastically out of effective range. It is believed that this mechanism may be important in the behavior of plexiglas, which was almost immune from damage in water, but was very susceptible under the more intense forces created in cavitating mercury.

---

*These statements are meant to apply only to cavitation damage in relatively initial phases as observed in this investigation. As already mentioned, macroscopic fatigue failures have also been observed eventually (Cb - 1% Zr alloy).

**Or the ultimate tensile strength, to which it is approximately proportional.

Some other considerations which may be important are:

i) recovery time required by material between blows, since these may be imposed at a relatively high frequency,

ii) ratio of dynamic to static mechanical properties of material, and

iii) corrosivity of material in fluid in question, which, although negligible under static conditions may become important under cavitating conditions.

B. Experimental Results

All the applicable quantitative experimental data, available to date from the present investigation, has been normalized to stainless steel under the same duration and flow conditions.[4] These individual data points for each material and fluid have then been averaged in such a manner that the averages were weighted according to quantity of damage in terms of mean depth of penetration. The normalized values were then plotted against ultimate strength, yield strength, Brinell hardness, and strain energy to failure, respectively. These plots are very preliminary, since much data is yet to be gathered. However, the plots show the large magnitude of data scatter, and indicate that, of the parameters used, the most successful correlation is achieved with strain energy to failure. Since hardness and yield strength are more or less proportional to ultimate strength for the materials used, only the plots for ultimate strength and strain energy to failure are presented (Figures 29 and 30). The correlation of averaged points to strain energy is quite good

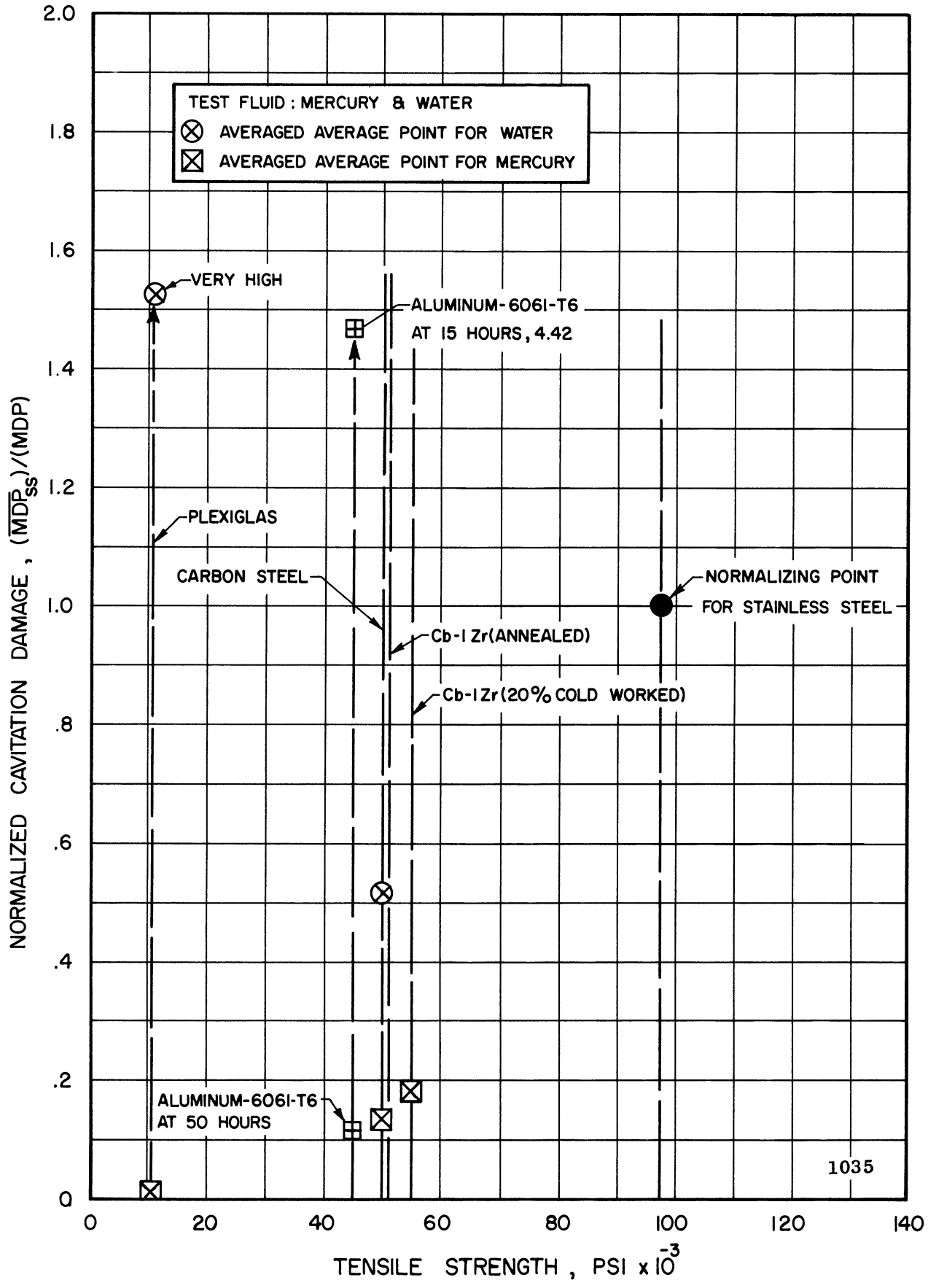

Figure 29. Normalized Cavitation Damage vs. Tensile Strength Comparison of Mercury and Water Data.

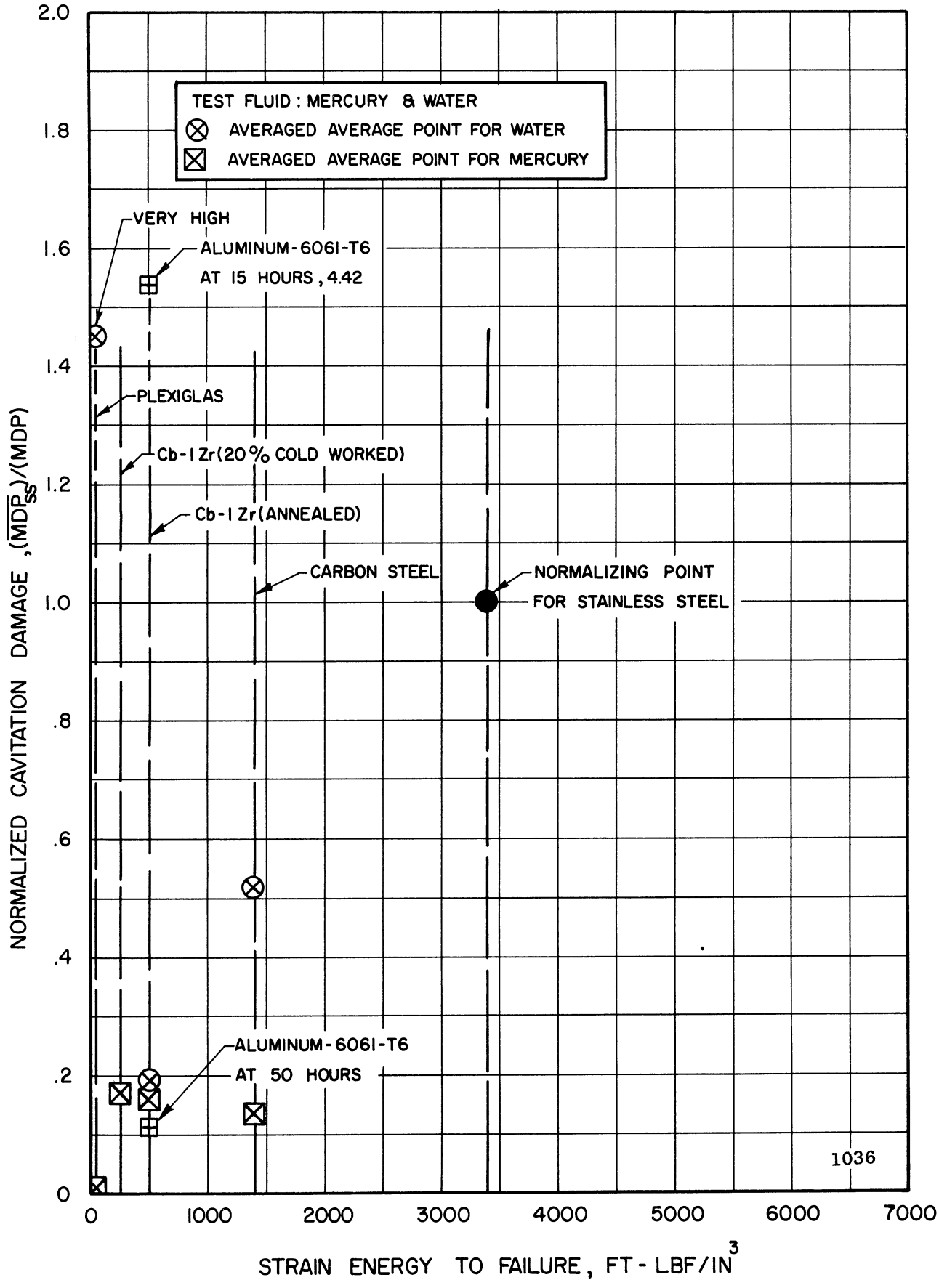

Figure 30. Normalized Cavitation Damage vs. Strain Energy to Failure, Comparison of Mercury and Water Data.

except for plexiglas in water, where as previously mentioned, mechanisms not considered in the choice of correlating parameter are believed involved. However, the scatter of individual points is very large, so that a prediction of damage a priori from such a correlation might not be meaningful. It is believed that a good correlation can only be achieved in terms of more complex groupings of material properties which consider more completely the mechanisms involved.

V. CONCLUSIONS

The following conclusions appear to be the most significant:

i) The detailed characteristics of the pitting observed on test specimens inserted into the diffusing portion of a cavitating venturi, depend significantly upon degree of cavitation, fluid, and material. The observed trends are generally explainable in terms of the hypothesized mechanisms.

ii) While the distribution of crater-type pits is essentially locally random in the early phases of cavitation damage, it becomes a function of the previous damage as this becomes sufficient to cause perturbations in the flow pattern. The local distribution of irregularly shaped pits, on the other hand, is often a function of surface imperfections, grain boundaries, etc.

iii) Although the early damage is composed of individual, generally non-overlapping pits, gross macroscopic fatigue-failure has eventually been observed for at least one material.

iv) The effects of throat velocity upon quantity of damage in the cavitating venturi is much less than previously supposed. In some cases damage decreases with an increase of velocity.

v) The damage with mercury in the cavitating venturi is the order of 100 times greater than that with water for the same range of velocity, so that mercury tests provide an accelerated cavitation test, perhaps midway between a conventional flowing system and an ultrasonic device.

vi) Of the conventional mechanical material properties, damage from the present tests is best correlated by strain energy to failure. However, the scatter of individual data points about the best curve is very large.

VI. REFERENCES

1. Hammitt, F. G. "Observations on Cavitation Damage in a Flowing System." Trans. ASME, J. Basic Eng., Series D, V. 85, No. 3, September 1963, pp. 347-359.

2. Hammitt, F. G., et al. "On Transient Loading Effects in Cavitation Pitting." ASME Paper to be presented at 1963 Annual Winter Meeting of ASME, November, 1963.

3. Hammitt, F. G., et al. "Cavitation Damage Tests with Water in a Cavitating Venturi," ORA Report No. 03424-4-T, Nuclear Engineering Department, The University of Michigan, (April, 1962).

4. Hammitt, F. G., et al. "Cavitation Damage Tests with Mercury and Water in a Cavitating Venturi and Other Components." ORA Report No. 03424-9-T, Nuclear Engineering Department, The University of Michigan, (September 1963).

5. Lichtman, J. Z., "Possible Contributions of Reentrant Flow to Cavitation Erosion." ASME Paper No. 62-HYD-3.

6. Kelly, R. W., Wood, G. M., Marman, H. V., Milich, J. J., "Rotating Disk Approach for Cavitation Damage Studies in High Temperature Liquid Metal." ASME paper presented at Hydraulics Division Meeting, (May, 1963).

7. Knapp, R. T., "Accelerated Field Tests of Cavitation Intensity." Trans. ASME, Vol. 80, No. 1, (Jan. 1958) 91-102; and "Recent Investigations of the Mechanics of Cavitation and Cavitation Damage." Trans. ASME, (Oct. 1955), 1045-1054.

8. Hobbs, J. M., "Problems of Predicting Cavitation Erosion from Accelerated Tests." ASME Paper No. 61-HYD-19.

9. Personal communication from A. Thiruvengadam to F. G. Hammitt.

10. Barinka, L. L., Hammitt, F. G., "Detailed Investigation of Cavitation Pitting Characteristics from Cavitating Venturi Tests." ORA Report No. 03424-8-T, Nuclear Engineering Department, The University of Michigan, (April, 1963).

11. Thiruvengadam, A., "A Unified Theory of Cavitation Damage," ASME Paper No. 62-WA-118.

VII. APPENDIX

SPECIFICATION OF CAVITATION CONDITIONS

The cavitation condition for all tests is defined in terms of "degree of cavitation", referring (except for initiation) to the extent of the cavitating region in the venturi.

i) Sonic Initiation - First sonic manifestation beyond that of single phase flow. This was detected either by ear or, in the earlier water tests, by using a piezoelectric crystal. The results of these two methods were approximately the same. In all cases sonic initiation occurred at a higher throat pressure than visible initiation.

ii) Visible Initiation - First appearance of a more or less complete ring of cavitation. This always appeared first at the throat exit.

iii) Cavitation to Nose - The approximate location of the termination of the cavitation region is at the upstream nose of the test specimen.

iv) Standard - The approximate location of the termination of the cavitation region is at the center of the test specimen.

v) Cavitation to Back - The approximate location of the termination of the cavitation region is at the downstream end of the test specimen.

vi) First Mark - The approximate location of the termination of the cavitation region is about 1-3/4 inches downstream from the throat outlet.

vii) Second Mark - The approximate location of the termination of the cavitation region is about 3-1/2 inches downstream from the throat outlet.

The location of these termination points is shown to scale in Figure 1. Although the termination is not sharp, the cavitation conditions can be quite precisely reproduced.